iScience

CellPress
OPEN ACCESS

Article

Spatiotemporal patterning of acoustic gaze in echolocating bats navigating gaps in clutter

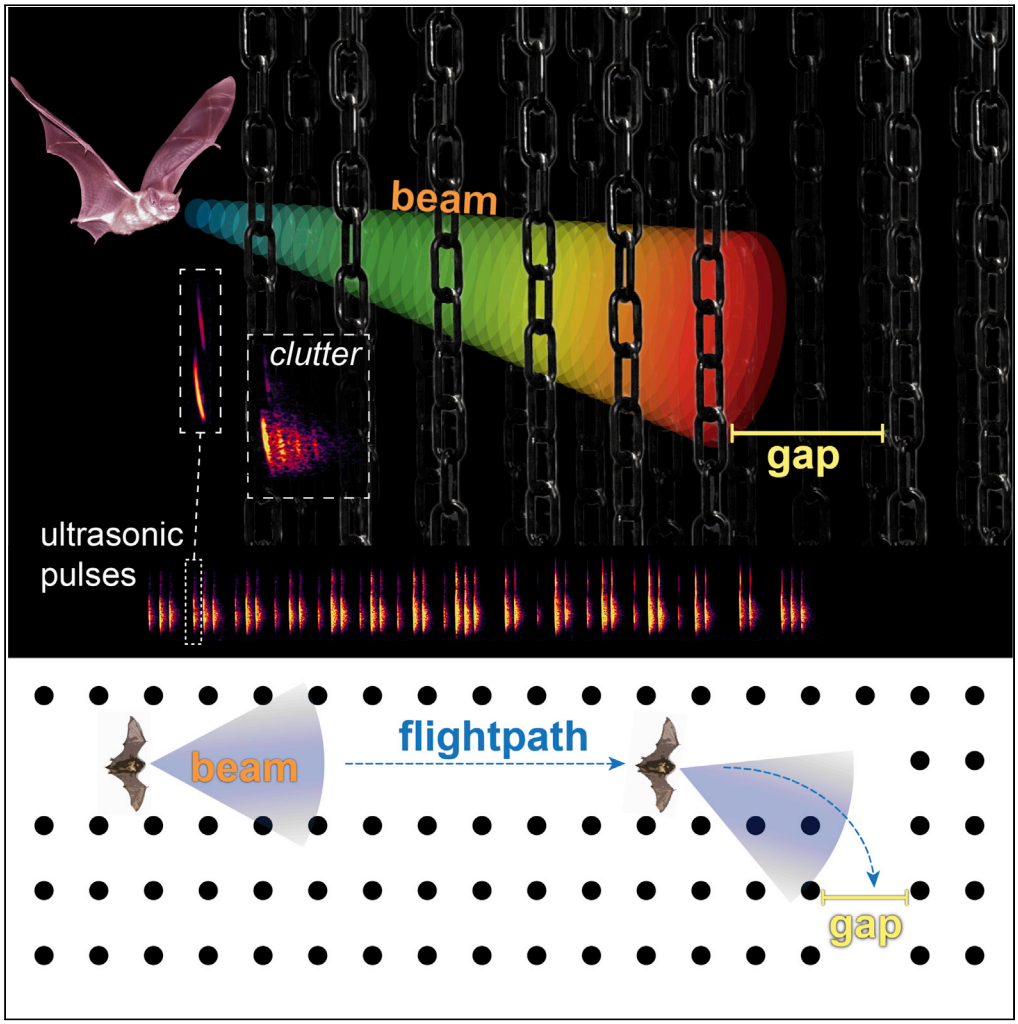

Amaro Tuninetti, Chen Ming, Kelsey N. Hom, James A. Simmons, Andrea Megela Simmons

andrea_simmons@brown.edu

Highlights

Echolocating bats use sonar to identify flightpaths through dense, cluttered scenes

Bats learn new flightpaths by switching beam aim before encountering obstacles

Bats see their environment in depth

Tuninetti et al., iScience *24*, 102353
April 23, 2021
https://doi.org/10.1016/j.isci.2021.102353

iScience

CellPress
OPEN ACCESS

Article

Spatiotemporal patterning of acoustic gaze in echolocating bats navigating gaps in clutter

Amaro Tuninetti,[1] Chen Ming,[2,3] Kelsey N. Hom,[1,4] James A. Simmons,[2,3] and Andrea Megela Simmons[1,2,3,5,*]

SUMMARY

We challenged four big brown bats to maneuver through abrupt turns in narrow corridors surrounded by dense acoustic clutter. We quantified bats' performance, sonar beam focus, and sensory acquisition rate. Performance was excellent in straight corridors, with sonar beam aim deviating less than 5° from the corridor midline. Bats anticipated an upcoming abrupt turn to the right or left by slowing flight speed and shifting beam aim to "look" proactively into one side of the corridor to identify the new flightpath. All bats mastered the right turn, but two bats consistently failed the left turn. Bats increased their sensory acquisition rate when confronting abrupt turns in both successful and failed flights. Limitations on biosonar performance reflected failures to switch beam aim and to modify a learned spatial map, rather than failures to update acquisition rate.

INTRODUCTION

Echolocating bats intercept flying prey and navigate through their environments using information provided by reflected echoes. To identify obstacles and open flightpaths, they actively modulate the number, temporal patterning, and spatial direction of their biosonar calls (Griffin, 1958; Moss and Surlykke, 2001; Surlykke and Moss, 2000). Many bat species forage and navigate in noisy, highly echoic (cluttered) environments, such as vegetation, forests, and caves (Schnitzler and Kalko, 2001), that challenge their biosonar system to decipher multiple, dynamic streams of echoes from numerous objects located at different distances. In these noisy environments, bats maintain flightpaths, detect specific (prey) objects in surrounding (non-prey) background clutter, identify particular echoes in multiple overlapping streams of echoes, and selectively attend to relevant echoes amid a stream of irrelevant ones that constitute the clutter (Amichai and Yovel, 2017; Beetz et al., 2019; Fujioka et al., 2014; Hiryu et al., 2010; Knowles et al., 2015; Melcón et al., 2011; Petrites et al., 2009; Sändig et al., 2014; Surlykke et al., 2009; Wheeler et al., 2016). The experiments described here analyze how one species of FM (frequency-modulated) bat, the big brown bat, *Eptesicus fuscus*, modifies the direction and timing of its biosonar calls when flying through a cluttered environment requiring maneuvers through tight turns. As in natural clutter, multiple objects in this environment are located nearer than the upcoming opening in the scene, so the bat has to peer through a screen of echoes to discern the place where a turn will be necessary to maintain the flightpath.

Big brown bats have a versatile biosonar system. They capture prey in open spaces as well as on the ground and in or near vegetation; they fly above the forest canopy, between gaps in foliage, and within caves and other roosting spots (Simmons, 2005; Simmons et al., 2001). Their sonar beam is wide (−6 dB beam width = 55°) and ensonifies a large acoustic field of view (Ghose and Moss, 2003; Hartley and Suthers, 1989). Because wide beamwidths result in echoes returning from all objects within the ensonified field of view, identifying target echoes and then developing a flightpath to maneuver around obstacles or capture a prey item within foliage is not a simple task. Echoes arriving from objects located near the periphery of the sonar beam can mask echoes from objects located near the front (Bates et al., 2011). To contend with this masking problem, big brown bats flying toward a target in an open room sequentially scan their surroundings to center the sonar beam on the target; they then lock onto the target several hundreds of milliseconds before physically approaching it (Surlykke et al., 2009). When navigating down straight corridors surrounded by dense acoustic clutter, they align the center of the beam with the direction of flight, with minimal side-to-side scanning throughout the duration of the flight (Knowles et al., 2015; Warnecke et al., 2016, 2018). It is not known how bats modify the direction of beam aim and their scanning behavior in highly cluttered environments requiring complex flightpaths. Understanding how bats make these modifications in different environments can elucidate the strategies they use to choose open flightpaths and to

[1]Department of Cognitive, Linguistic, & Psychological Sciences, Brown University, Providence, RI 02912, USA

[2]Department of Neuroscience, Brown University, Providence, RI 02912, USA

[3]Carney Institute for Brain Science, Brown University, Providence, RI 02912, USA

[4]Present address: PhD Program in Biology, Graduate Center, CUNY, New York, NY 10016, USA

[5]Lead contact

*Correspondence: andrea_simmons@brown.edu

https://doi.org/10.1016/j.isci.2021.102353

reject surrounding clutter echoes, and when these strategies might fail (Kounitsky et al., 2015; Grief et al., 2017).

Besides changing beam aim, big brown bats also modify their sensory acquisition rate when flying in cluttered environments compared to flying in the open (Moss et al., 2006; Surlykke and Moss, 2000). In the presence of clutter, bats increase their rate of call (pulse) emission to update their view of the acoustic scene. However, at increased pulse rates, the bat emits a new pulse before all the echoes created by the previous pulse have returned. This overlap in emitted pulses and returning echoes produces pulse-echo ambiguity, the problem in determining which echo corresponds to which emitted pulse and thus in calculating the distance to the specific object that created that echo (Denny, 2007). One way of solving this ambiguity problem is to emit pulses in sonar sound groups (SSGs) of alternating short and long intervals between individual pulses or groups of pulses (Hiryu et al., 2010; Kothari et al., 2014; Moss et al., 2006). Indeed, in the corridor experiments described above, big brown bats emitted more grouped pulses when flying through narrower and more cluttered corridors (Accomando et al., 2018; Petrites et al., 2009; Wheeler et al., 2016). These behaviors are consistent with the hypotheses that changes in pulse timing occur when the bat needs to gather more frequent updates of the acoustic scene (Moss et al., 2006; Falk et al., 2014), and that the presence of SSGs provides an index of the perceptual difficulty of the task to the bat (Kothari et al., 2014; Lewanzik and Goerlitz, 2021; Petrites et al., 2009; Simmons et al., 2020).

One issue with the hypothesis that changes in pulse timing reflect the bat's own interpretation of an acoustic scene as "easy" or "difficult" is that in many flight and obstacle avoidance experiments, big brown bats exhibit excellent performance, with few or no errors (Hom et al., 2016; Knowles et al., 2015; Petrites et al., 2009; Simmons et al., 2018; Wheeler et al., 2016; but see Surlykke et al., 2009). They navigate successfully down straight and curved corridors, as narrow as 40 cm (their wingspan is only 32–35 cm), surrounded by arrays of hanging plastic chains producing dense, extended streams of echoes (Accomando et al., 2018; Petrites et al., 2009; Wheeler et al., 2016), even after exposure to intense levels of noise that would be expected to alter their sensitivity to echoes (Hom et al., 2016; Simmons et al., 2018). Here, we designed a flight task where big brown bats were required to maneuver down a narrow corridor surrounded by acoustic clutter produced by reflective chains and then through abrupt 90° turns. This experimental paradigm broadly mimics an acoustic scene these animals would experience when attempting to locate and fly through gaps between foliage. We made three predictions. First, the inclusion of abrupt turns makes the task challenging for bats to master. Second, bats alter the direction of their beam aim to ensonify the area surrounding the turns well before physically reaching them, and these changes in beam aim are related to performance. Finally, bats call at high rates with pronounced pulse grouping as they approach the turn, and these changes in pulse grouping are related to performance.

RESULTS

Four big brown bats were challenged to fly through a 40-cm-wide corridor surrounded by an array of 217 hanging plastic chains that produced intense, extended echoes (acoustic clutter; see transparent methods). Two of these corridors incorporated sharp 90° right or left turns into the flightpath (Figure 1). The task required the bat to detect the open gap in the chain array and then perform an abrupt flight maneuver to navigate through it and receive a reward. Bats completed 7 days of flights in the Straight corridor condition, 9 days in the Right Turn condition, and 6–7 days in the Left Turn condition. Two bats (Bat 3 and Bat 4) also completed 1 day of flights in a Reversed Right Turn condition.

Performance

We defined a successful flight as one in which the bat flew the entire corridor length to the appropriate wall without turning around or exiting the corridor through the chains, landing on a chain, or falling to the floor. Percent successful flights (Figure 2) varied significantly with task condition [one-way analysis of variance: $F(2,42) = 34.21$, $p < 0.001$] and among bats [$F(3,21) = 13.09$, $p < 0.001$]. All bats flew through the Straight corridor with few errors [mean (M) percent correct = 94.2%, N = 420 flights]. Over seven days of flights, the mean success rate increased from 91% on the first day of flights to 100% on the last day of flights. Performance of previously experienced (Bats 1 and 4) and previously naive (Bats 2 and 3) was similar (M = 96.7% and 91.8%, respectively).

Performance in the Right Turn condition (M = 86.9%, N = 545 flights) did not differ significantly from that in the Straight condition (pairwise comparisons: $p = 0.096$). All four bats, regardless of whether they had

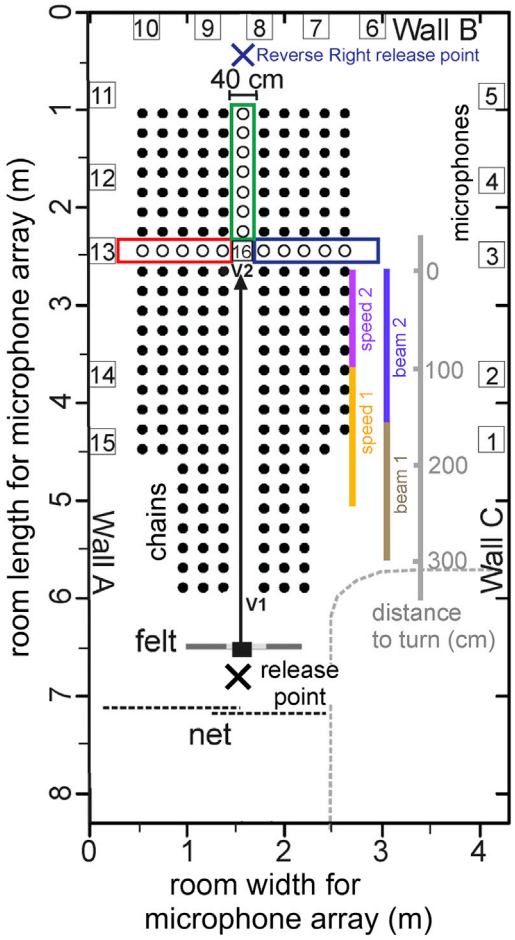

Figure 1. Diagram of the flight room and chain array

Dimensions of the flight room (m; left y and x axes) and the location of the hanging chains (filled circles) are shown. Bats were released through an opening in hanging felt (small filled rectangle) at the release point (black X) and flew down a corridor (40 cm width) through the chain array. Chains were hung in rows and columns 20 cm apart. In the Straight condition, chains were removed (open circles) from the section outlined in green, and both the red and blue sections were blocked with chains. Bats were rewarded for landing on Wall B. In the Right Turn condition, chains were removed from the blue section of the chain array, and the green and red sections were blocked with chains. Bats were rewarded for landing on Wall C. In the Left Turn condition, chains were removed from the red section, and the blue and green sections were blocked with chains. Bats were rewarded for landing on Wall A. In the Reversed Right Turn condition, bats were released from the blue X on Wall B and flew through the green and red sections, landing on Wall A. The blue section was blocked by chains. The colored lines on the right side of the array marked beam 1 (brown) and beam 2 (dark purple) show the two segments of the flightpath used for calculating beam aim. These two segments are referred to distance from the turn, as shown by the gray numbers; the turn is at 0 cm and the beginning of measured flightpath is at 300 cm. The colored lines marked speed 1 (orange) and speed 2 (purple) show the two segments of the flightpath used to calculate flight speed. Small numbered boxes around the perimeter of the room show the locations of recording microphones, and boxes labeled "v" show the position of recording cameras. Black dotted lines indicate a net that prevented the bat from flying into the rest of the room, and recording equipment was located behind the curved gray dotted line.

previous laboratory experience in flying amid clutter, experienced a large drop in performance on the first day of the Right Turn condition, with success rate ranging from 0% to 69% (M = 45.1%). Success rate reached M = 84.8% within the first 3–4 days of this condition (Figure 2). Experienced and naive bats had similar success rates (M = 83.9% and 89.9%, respectively).

Success rate in the Left Turn condition differed considerably among bats. Bat 1 and Bat 2 improved their performance over flight days, with success rate increasing from M = 26.5% on the first day of flights to M =

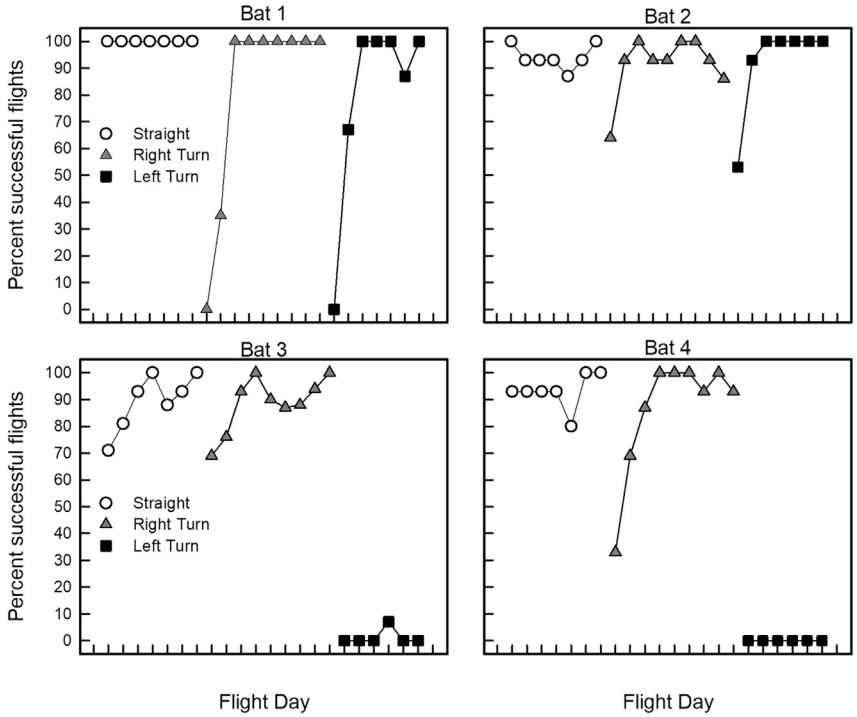

Figure 2. Performance of individual bats on each flight day in the three different task conditions

Bats performed 15–18 flights per day. All bats showed improved performance (increased percentage of successful flights) with experience in Right Turn flights; only two bats showed improved performance with experience in Left Turn flights.

100% on the last day of flights. On the other hand, neither Bat 3 nor Bat 4 completed the task successfully, with success rates of 0% on both the first and the last day of flights.

We statistically analyzed performance on a bat-by-bat basis. Bat 1 and Bat 2 both showed similar performance across conditions [$F(2,18) = 1.13$, $p = 0.35$; $F(2,20) = 0.11$, $p = 0.90$, respectively]. Conversely, Bat 3's performance differed significantly across conditions [$F(2,19) = 204.89$, $p < 0.001$]. This bat performed equally well in the Straight and Right Turn conditions (pairwise comparisons: $p = 0.85$), but significantly worse in the Left Turn compared with Right Turn condition (pairwise comparisons: $p < 0.001$). Bat 4's performance also differed significantly across conditions [$F(2,19) = 78.06$, $p < 0.001$]. This bat performed similarly in the Straight and Right Turn conditions (pairwise comparisons: $p = 0.36$), but significantly worse in the Left Turn compared with the Right Turn condition (pairwise comparisons: $p < 0.001$).

Bat 3 and Bat 4 completed 1 day (N = 39 flights) in the Reversed Right Turn condition, with a success rate of 80% correct. Because of the small sample size in this condition, these data were not included in subsequent statistical analyses.

Beam aim

We quantified beam aim using cross-correlation and time-difference-of-arrival of calls recorded by 14 microphones (see transparent methods). We calculated beam aim angles (M, SD; Table 1) in successful flights by individual bats in each flight condition for two portions of the flightpath (Figure 1): 300 to 150 cm before the turn (beam 1, brown) and 150 to 0 cm before the turn (beam 2, dark purple). Mean (M) beam aim was calculated in 10-cm bins. Mean beam aims (+/− 1 SD) in all successful Straight, Right Turn, and Left Turn flights are plotted in Figures 3A–3C.

In the Straight condition (Figure 3A), beam aims of all bats remained centered around 0° throughout the flightpath, with a mean deviation from midline toward the left of −1.03° (beam 1) and −1.79° (beam 2). There is no statistical difference in beam angle between the two experienced and the two naive bats for either beam 1 or beam 2 (Welch two-sample t test, $p = 0.14$ and 0.62, respectively). In the Right Turn

Table 1. Beam aim angles in all successful flights for each bat

Condition	Distance to turn		Bat 1	Bat 2	Bat 3	Bat 4
Straight	300 cm–150 cm	N	*1,895*	841	1,101	*1,744*
		M	*−1.25°*	0.39°	1.74°	*3.27°*
		SD	*8.12°*	6.73°	5.98°	*8.23°*
	150 cm–0 cm	N	*1,222*	696	775	*975*
		M	*−3.87°*	−3.66°	−0.43°	*0.77°*
		SD	*6.17°*	6.40°	6.13°	*9.50°*
Right Turn	300 cm–150 cm	N	*2,464*	648	1,522	*2,735*
		M	*3.95°*	−2.62°	2.37°	*2.38°*
		SD	*8.85°*	6.91°	6.69°	*7.39°*
	150 cm–0 cm	N	*2,082*	937	1,929	*1,953*
		M	*27.88°*	16.49°	28.11°	*25.08°*
		SD	*27.55°*	27.61°	27.08°	*27.07°*
Left Turn	300 cm–150 cm	N	*1,695*	379	–	
		M	*−3.46°*	0.17°	–	–
		SD	*12.52°*	9.78°	–	–
	150 cm–0 cm	N	*1,506*	656	–	
		M	*−26.55°*	−20.56°	–	–
		SD	*26.74°*	18.77°	–	–

N = number of angles, M = mean, SD = standard deviation. Flightpath is divided into two: 300–150 cm (beam 1, brown line, Figure 1) and 150–0 cm (beam 2, dark purple line, Figure 1) before the 90° turn (or equivalent for Straight flights). Empty cells indicate no data for that combination of bat and condition. Italicized values are from the two bats that were experienced in flight tasks.

condition (Figure 3B, Table 1), mean angles for beam 1 were +1.52° away from midline toward the right; this increased to a mean of +24.39° for beam 2, as the bats aimed their beams toward the right edge of the corridor. The two experienced bats had larger beam angles (i.e., shifted more toward the right) than the two naive bats ($p < 0.0001$ for both beam 1 and beam 2). We then examined when during the 150–0 cm segment of the flightpath (beam 2) that bats first began to aim toward the Right Turn. We chose as the criterion the first point at which the beam angle at beam 2 was more than 1 SD away from the mean angle for beam 1. These rightward shifts occurred at 60 cm (Bat 1), 30 cm (Bat 2), 60 cm (Bat 3), and 65 cm (Bat 4) from the turn point. In the Left Turn condition (Figure 3C, Table 1), beam aim 1, averaged over the two successful bats, was −1.65° toward the left edge of the corridor. Mean angle for beam 2 increased to −23.55° toward the left. The experienced bat (Bat 1) had larger beam angles (i.e., more to the left) than the naive bat (Bat 2) for both beam 1 and beam 2 ($p < 0.001$). Using the same criterion described above, beam aim shifted toward the left 40 cm (Bat 1) and 60 cm (Bat 2) before the bat physically reached the turn.

Beam aim angles on failed flights are summarized in Table S1. In Straight failed flights, beam aim angles over all four bats are larger (M = 5.29° and 3.45°, beam 1 and beam 2, respectively), indicating greater deviation from the midline, than those in successful flights (Table 1). Beam angles in failed Right Turn flights for beam 1 was close to the midline (M = +1.45°) and increased to M = +21.86° for beam 2. This shift to the right is smaller than that in successful Right Turn flights (Table 1), indicating that bats did not aim their beams as effectively toward the right edge of the corridor. In failed Left Turn flights, beam aim averaged over all four bats remained at the midline (M = +0.49°) for beam 1, but switched to the right, rather than the left, side of the corridor for beam 2 (M = +15.63°). In other respects, beam aim was part of the overall behavior of failed flights, which entailed the bat not flying along the corridor but leaving it or landing on the floor, which coupled flight and beam in a manner difficult to untangle.

We then asked if beam aim before the turn (150–0 cm, beam 2) differed between the beginning and the end of flights in the three conditions. We plotted the beam aim of all calls in this portion of the flightpath for all flights (both successful and failed) on the first day and on the last day of each condition (Figure 4). Beam angles in failed flights are plotted in Figure S1. We calculated the linear regression through the

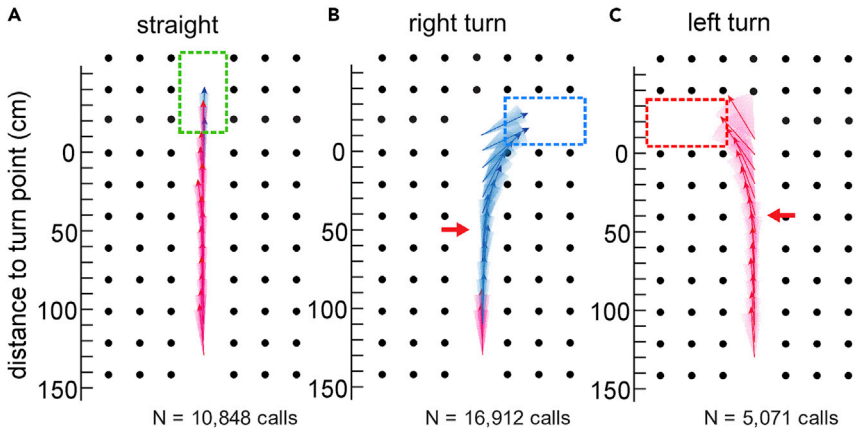

Figure 3. Mean and standard deviation (SD) of beam aim of all calls emitted in successful flights

(A–C) (A) Straight flights; (B) Right Turn flights; (C) Left Turn flights. The y axis shows the portion of the flightpath (see beam 2 line, Figure 1) immediately before the turn (or equivalent point in Straight flights). The position of the turn (or equivalent location in straight flights) is shown by the green, blue, and red dashed rectangles in (A, B, and C), respectively. Filled circles show the positions of hanging chains in each condition. Colored vectors plotted along the midline of the chain array show mean beam aim calculated in 10-cm bins. Colored envelopes around these vectors show the SD within each window. Blue vectors denote positive beam aims >0°, red vectors denote negative beam aims <0°. N = Numbers of calls used to calculate beam aim. In (B and C), red horizontal arrows denote the area in which beam aim diverges more than 1 SD from the midline.

data from all flights on each of these 2 days and compared the slopes of the regression lines. In the Straight condition, beam aim slope did not differ significantly (Bonferroni-corrected $\alpha = 0.004$) between the first and last day of flights for any bat [Bat 1: $F(1,330) = 1.6$, $p = 0.21$; Bat 2: $F(1,325) = 0.94$, $p = 0.33$; Bat 3: $F(1,267) = 1.30$, $p = 0.26$; Bat 4: $F(1,352) = 0.54$, $p = 0.46$]. Bats aimed their beam within $\pm 5°$ of the midline on both days.

All bats successfully navigated the Right Turn. On the first day of Right Turn flights, Bat 1 emitted most calls straight ahead, centered around 0° (Figure 4, center column). On the final day, Bat 1 shifted its beam aim toward the right, with the regression intercept at +45° [significantly different than the first day: $F(1,467) = 107.8$, $p < 0.0001$]. Bat 2's beam aim did not differ significantly between the first and last days of Right Turn flights [$F(1,272) = 5.2$, $p = 0.02$], because its beam on the first day of flights had already shifted toward the Right Turn. Bat 3 also shifted its beam toward the right on the first day of Right Turn flights, and showed even more pronounced shifts on the last day, to an angle of +45° [$F(1,408) = 8.7$, $p = 0.003$]. Bat 4 aimed its calls on the first day toward the right (regression intercept of +21°), with a more pronounced shift on the last day [regression intercept of +45°; $F(1,497) = 61.7$, $p < 0.0001$]. Note that on the final day of Right Turn flights, three bats continued to emit a small number of calls toward the front ($\pm 10°$) or to the left ($< -10°$) within 30 cm of the Right Turn (Bat 1: 11 calls, Bat 2: 6 calls, Bat 3: 1 call, Bat 4: 0 calls). Even on failed Right Turn flights (Figure S2), the beam is generally aimed toward the right, with considerable scatter.

Differences in performance among bats in the Left Turn condition are reflected in their beam aims (Figures 4 and S1). The third column in Figure 4 shows the calls emitted by each bat on the first day after switching from the Right Turn to the Left Turn condition. Bat 1 emitted its calls toward the center of the corridor on the first day of flights, whereas on the final day its beam aim had shifted in the direction of the Left Turn, at an angle of −19° [significantly different from the first day: $F(1,555) = 39.3$, $p < 0.0001$]. Bat 2 also emitted its calls toward the center during the first day of Left Turn flights, whereas on the final day it shifted its beam toward the left at an angle of −36° [$F(1,285) = 52.6$, $p < 0.0001$]. In contrast, Bat 3 emitted most of its calls toward the right on the first day, at an angle of +9°, and shifted to the left at an angle of −6° on the final day [$F(1,376) = 36.6$, $p < 0.0001$]. This shift was toward the correct direction, but it was not large enough to guide the bat through the Left Turn successfully. Bat 4 aimed its beam slightly toward the left (−9°) on the first day of this condition, but on the last day it aimed its beam to the right at an angle of +9° [not significantly different: $F(1,347) = 3.2$, $p = 0.07$]. This failure to switch beam aim to the appropriate direction (see also Figure S1) is consistent with this bat's behavioral failure to navigate the Left Turn

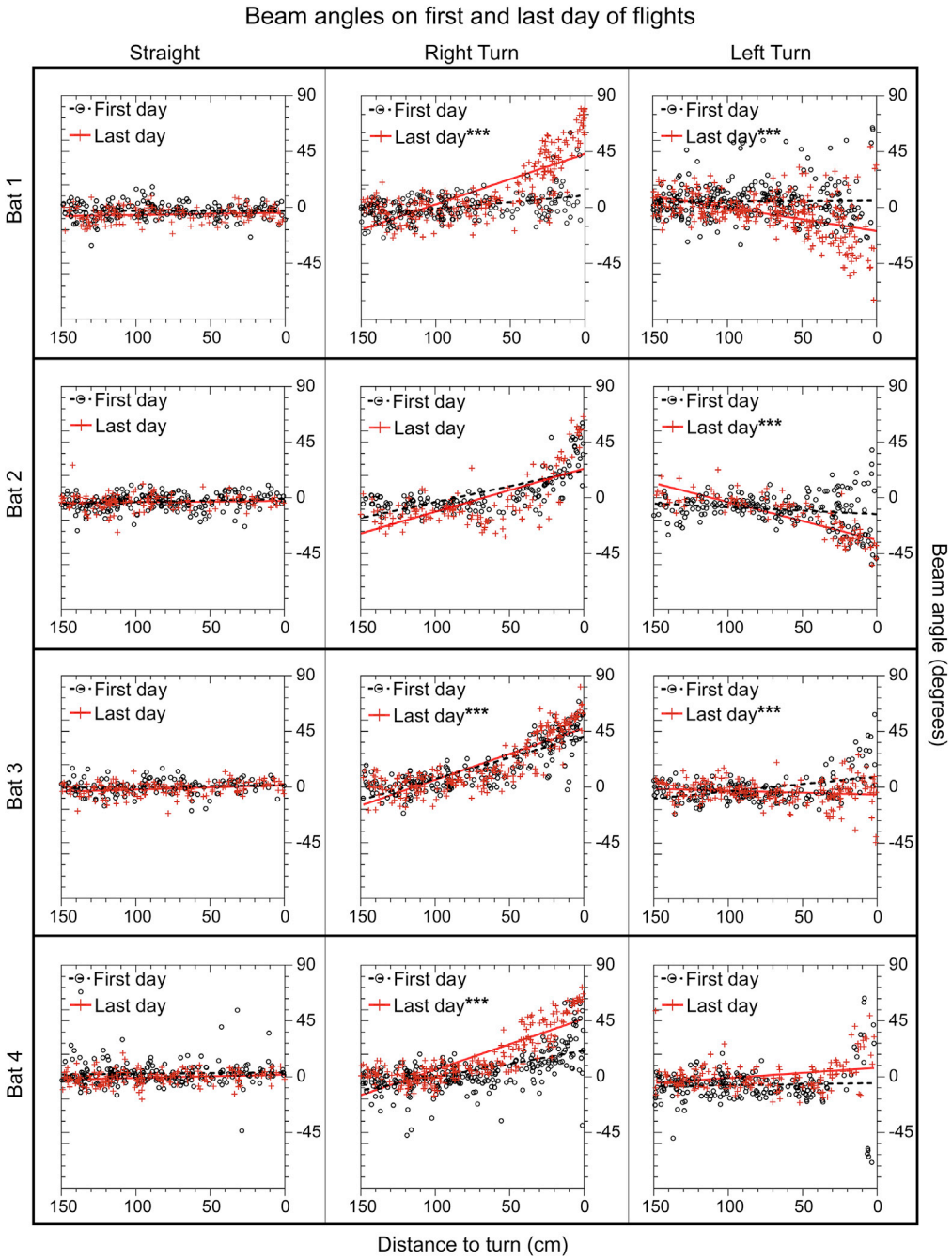

Figure 4. Beam angle of calls emitted from 150–0 cm before the turn (or equivalent location in Straight flights) on first and last day of each flight condition

Each panel shows beam angles for the first day of flights in that condition (open black circles), beam angles for the last day of flights in that condition (red crosses), and regression lines (first day, black; last day, red) through the data points. Distance to the turn (150–0 cm) is shown on the x axis. y Axis shows beam angle (positive values show shifts toward the right, negative values show shifts toward the left). Asterisks next to "Last day" indicate that beam aim regression in the final day was significantly different from that in the first day. Plots show beam aim values from both successful and failed flights, with the exception of Left Turn flights for Bats 3 and 4, which show values from failed flights only.

(Figure 2). All bats directed some calls straight ahead (±10°) or to the right (>10°) within 30 cm of the turn on the last day of the Left Turn condition (Bat 1: 20 calls, Bat 2: 1 call, Bat 3: 43 calls, Bat 4: 25 calls).

Flight speed

We measured bats' flight speeds (see transparent methods) over the portion of the flightpath before they reached the turn (or equivalent point in Straight flights). We separated this portion into two—a farther segment (250–100 cm before the turn; speed 1, orange line, Figure 1) and a nearer segment (100–0 cm before the turn; speed 2, purple line, Figure 1). The nearer segment (0–100 cm before the turn) was chosen for flight speed measurements because individual bats diverted their beam angle away from the midline at various points between 0 and 100 cm from the turn (see Figure 4), indicating that the bats began physically preparing for the turn within 100 cm from the turn. The farther segment (250–100 cm) was chosen as the comparison range, as this segment was most representative of the bat's stable flight speed in the straight section of the turn conditions; distances farther than 250 cm from the turn were excluded to avoid variable flight speeds due to the bat's initial release. Median flight speed in the farther segment of the Straight corridor differed among bats, from a high of 3.1 m/s for Bat 1 to a low of 2.6 m/s for Bat 3. All bats flew slower in the farther segment of the Turn corridors, with median flight speeds of 2.4 to 2.2 m/s (Figure S2). Flight speeds in the nearer segment of the Straight corridor were consistently lower than in the farther segment, varying from a high of 2.9 m/s for Bat 1 to a low of 2.2 m/s for Bat 3. All bats significantly decreased flight speeds (to 1.8–2.0 m/s) in the nearer segment of the Turn corridors (Kolmogorov-Smirnov tests, $p < 0.001$). Flight speeds could not be calculated in failed flights, because bats aborted these flights at different locations in the corridor.

Call timing

We calculated inter-pulse intervals (IPI), the time between each individual pulse, for all calls emitted during flights. To quantify how the bats modified their call timing in the three flight conditions, we fit IPI values from successful flights to two separate linear mixed effects models (LMMs). We also categorized calls into SSGs to compare pulse clustering in the three conditions. We plotted IPI data from both successful and failed flights as distributions of pre- and post-IPI in order to highlight qualitative differences in the timing strategies used by individual bats in relation to their behavioral performance.

Linear mixed effects models

We predicted that bats would decrease IPIs as they approached the turn point, as the area, particularly the depth, that is acoustically visible to them shrinks. We also predicted that IPIs would increase over time within each of the three flight conditions, as the bats became more accustomed to the spatial layout and less dependent on perceptual information regarding their immediate surroundings. To test these predictions, we fit the IPI timing data (defined as the post-IPI value, i.e., the time interval after each pulse) to two LMMs. The first LMM tested whether linear relationships exist in how IPIs changed as the bats approached the turn (or the equivalent point in Straight flights), as well as how these relationships differ among individual bats and different task conditions. Only IPIs of calls emitted before entering the turn (or the equivalent location in Straight flights) were input into the model. Three fixed effects were included: Condition (Straight, Right Turn, or Left Turn), Number of Calls, and the interaction of those two effects. The variables Trial Number, Day number, Condition, and Bat were added as nested random effects. Table 2 shows the results of this model, and Figure 5A shows the model's predicted regression lines of change in IPI as the bats approached the turn (or equivalent point) in each condition. IPI values in successful flights did not differ significantly among conditions ($p > 0.05$). Mean IPIs from each individual bat varied from 27–35 ms in the Straight condition, 27–28 ms in the Right Turn condition, and 25–41 ms in the Left Turn condition. (In contrast, over all failed flights by all bats, mean IPI ranged between 25 and 27 ms). The results of the LMM showed a significant interaction between Condition and Number of calls ($p < 0.001$; Table 2). IPI increased in the Straight condition as the bat approached the equivalent point where the turn was located in future conditions, by 0.08 ms per call (Figure 5A). Conversely, in the Right Turn condition, IPI decreased by 0.03 ms per call (significantly different than the increase in the Straight condition, $p < 0.001$). In the Left Turn condition, IPI decreased even more, by 0.14 ms per call (significantly lower than in both the Straight and Right Turn conditions, $p < 0.001$).

To determine whether the non-randomized order of flight conditions affected the results, we fit the IPI values to a second LMM, which analyzed the change in IPI as a factor of the number of experimental days the bat spent in that condition. This LMM includes fixed effects for Number of days and for the

Table 2. Results of the linear mixed effects model of IPI as the bat approaches a turn

Linear mixed effects model predicting post-IPI as bat approaches turn			
Predictors	Estimates	CI	p
(Intercept)	33.17	26.94–39.40	**<0.001**
Condition	−1.53	−3.82–0.75	0.189
Number of calls to turn	−0.19	−0.21–−0.17	**<0.001**
Condition × No. of calls	0.11	0.10–0.12	**<0.001**
Random effects	Variance		
σ^2	141.56		
Trial number	4.72		
Day number	3.14		
Condition	6.28		
Bat	20.74		
Total	176.44		
Observations	46,901		

CI, confidence interval. P values in bold are statistically significant.

interaction between Condition and Number of days. Table 3 shows the results from this LMM, and Figure 5B shows the model-predicted IPI over the nine flight days within the three consecutive conditions. There is a significant effect of condition ($p < 0.05$) and a significant Condition by Number of days interaction ($p < 0.001$; Table 2). IPIs in Straight flights increased significantly over days, by 0.84 ms per day ($p < 0.001$). In the Right Turn condition, IPIs also increased over days, by 0.29 ms, but significantly less than the increase in Straight flights ($p < 0.001$). Conversely, IPIs decreased by 0.25 ms per day in Left Turn flights (significantly different from Straight flights, $p < 0.05$).

Although the LMMs allow us to determine if there are linear trends over time or among conditions, they do not give detailed information about more complex, nonlinear temporal calling patterns. This includes the grouping of calls into SSGs, groups of two or more closely spaced calls flanked by longer IPIs. To categorize the bat's clustering of calls into groups, we implemented a previously described algorithm (Kothari et al., 2014) with revised criteria as used in experiments that included high-density clutter (Warnecke et al., 2016, 2018). An example of the output of this algorithm is shown in Figure 6 (successful Straight flight) and Figure S3 (successful and failed Right Turn flights).

We calculated the proportions of SSGs in successful and failed flights in all three flight conditions. Figure 7 and Table S2 show the relative proportion of calls in each condition identified as single calls or as SSGs of varying size. Data are shown for successful flights only, except for Bat 3 and Bat 4 in the Left Turn condition, which show data from failed flights. Bats emitted most of their calls in SSGs containing two or more calls as they approached the turn (or equivalent point in the Straight condition). The most common SSG was a doublet (proportions of 0.393–0.817), with triplets or single calls the second most common. A few calls were classified as SSGs of 7 or 8 pulses. In successful flights, changes in condition from Straight to Turn led to significant increases in the proportions of calls emitted as SSGs [Bat 1: Straight versus Right, $\chi^2_{(1,\ N\ =\ 9732)} = 656$, $p < 0.001$; Bat 1: Straight versus Left, $\chi^2_{(1,\ N\ =\ 8683)} = 815$, $p < 0.001$; Bat 2: Straight versus Right, $\chi^2_{(1,\ N\ =\ 8458)} = 1{,}906$, $p < 0.001$; Bat 2: Straight versus Left, $\chi^2_{(1,\ N\ =\ 5267)} = 1{,}605$, $p < 0.001$; Bat 3: Straight versus Right, $\chi^2_{(1,\ N\ =\ 10791)} = 589$, $p < 0.001$; Bat 4: Straight versus Right, $\chi^2_{(1,\ N\ =\ 11317)} = 407$, $p < 0.001$]. Consistent with the data from successful flights, the majority of SSGs in failed flights (Table S2; Bat 3 and Bat 4, Left Turn) were doublets. Bat 3 and Bat 4 emitted small proportion of pulses (0.004–0.041) in groups of 4 and 5, and Bat 4 emitted some groups of 6 and 7. For these two bats, the proportion of SSGs differed significantly between Right Turn and Left Turn conditions [Bat 3: Right versus Left, $\chi^2_{(1,\ N\ =\ 12586)} = 2{,}825$, $p < 0.001$; Bat 4: Right versus Left, $\chi^2_{(1,\ N\ =\ 13244)} = 1{,}247$, $p < 0.001$], with the difference due to production of more SSGs of 3–8 pulses.

The non-linear way in which bats modify the timing of their calls is also visualized by plots of the distribution of pre-IPI values of every call against the corresponding post-IPI values (Figure 8). These plots serve as a form of visual "fingerprint" highlighting the unique temporal pattern of call timing that each individual bat employed,

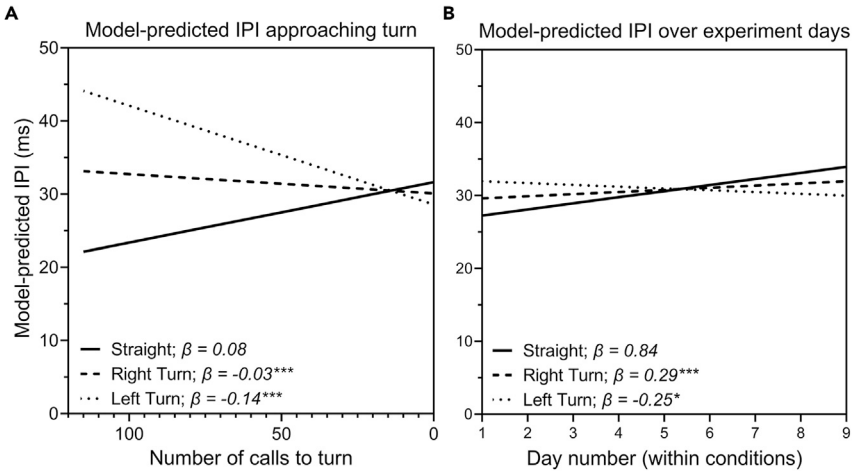

Figure 5. Results of linear mixed effects models

(A and B) Linear mixed effects model predictions of changes in IPI in successful flights as the bat approaches the turn (A) and as the bat completes multiple days of flights in the same condition (B). Asterisks indicate that slopes for the turn flights are significantly different from the slope for Straight flights.

despite all bats navigating the same physical environment. They are useful for displaying pulse clustering because they do not rely on a specific algorithm for defining SSGs; as shown previously, changing the algorithm produces different classifications (Kothari et al., 2014; Warnecke et al., 2016, 2018). Figure 8 shows that individual bats emitted calls with both long (>50 ms) and short (<50 ms) IPIs, but varying in such a way as to form dark clusters of values above and below the diagonal line (where pre-IPI = post-IPI). The diagonal line shows a 1:1 relationship between pre-IPIs and post-IPIs. Clustering of IPIs away from the diagonal shows that SSGs are present, although these plots cannot identify specific types of SSGs. Comparing plots between individual bats flying in the Straight condition (Figure 8, first column) shows that these clusters differ in their number and position across bats. Note that for Bat 3 and Bat 4, the clustering of pulses in their failed flights is similar to that in their successful flights (Figure 8, last column). These temporal fingerprints are consistent between flight conditions for an individual bat, although they do differ among bats.

DISCUSSION

Turning amid clutter is a difficult task

This experiment required big brown bats to navigate down narrow corridors and through sharp 90° turns embedded in intense acoustic clutter produced by a dense array of surrounding chains. We hypothesized that bats would find this task challenging, and our results support this hypothesis. Bats were able to fly down Straight corridors with a mean success rate of 94% (four bats). This high success rate is consistent with those found in other experiments that also challenged bats to navigate narrow straight or curved corridors surrounded by various densities of clutter (mean success rates of 93% [Hom et al., 2016], 94% [Simmons et al., 2018], 97% [Wheeler et al., 2016], and 95%–99% [Warnecke et al., 2016, 2018]). Adding abrupt 90° turns to the flightpaths decreased mean success rates to 84% (four bats) in the Right Turn condition and to 85% (two bats) in the Left Turn condition. A previous experiment challenging bats to fly through 40-cm openings in fine mist nests reported success rates of 50%–82% (Surlykke et al., 2009). In that experiment, bats were not required to make sharp turns, and the mist nets returned echoes that were less intense than those reflected by the chains in our experiment. Another experiment in which bats had to navigate past fine mist nests reported excellent performance (Knowles et al., 2015).

Bats were initially unable to adapt to a sudden change in flightpath, from Straight to Right Turn or from Right Turn to Left Turn, requiring 2 to 3 days (30–45 individual flights) to achieve final success. In the Right Turn condition, performance improved for all bats, reaching 100% correct in one animal, as they gained more experience with the flightpath over experimental days. After initial failures, two bats were able to achieve a success rate of 100% in the Left Turn condition; however, two other bats were unable to master that condition over the duration of the experiment, even with practice. These large individual differences indicate that the Left Turn was not intrinsically more difficult due to its closer proximity to the flight room wall. Moreover, bats' previous

Table 3. Results of the linear mixed effects model of IPI over consecutive days within conditions

Linear mixed-effects model predicting post-IPI over experimental days			
Predictors	Estimates	CI	p
(Intercept)	23.51	17.54–29.48	**<0.001**
Condition	2.89	0.76–5.02	**<0.05**
Day number	0.84	0.88–1.88	**<0.001**
Condition * Day No.	−0.54	−0.80–−0.28	**<0.001**
Random effects			
σ^2	142.86		
Trial number	4.39		
Day number	1.72		
Condition	4.08		
Bat	20.12		
Observations	46,901		

CI = confidence interval. P values in bold are statistically significant.

experience with flying down narrow corridors does not explain this individual variability; the same bat that achieved a high level of performance in earlier corridor experiments (Wheeler et al., 2016) had a success rate of 0% in the Left Turn condition, whereas a previously naive bat achieved a final success rate of 85%. It is possible that the two bats that failed to navigate the Left Turn could have learned it with even more experience, but this could not be tested as they were unwilling to continue flying in that condition. These same two bats were able to navigate a Reversed Right Turn condition, which attempted to control for proximity of the turn to the wall. However, this condition was run for only one day, rather than the 7–9 days of the other conditions, again due to the bats' refusal to continue flying. We cannot determine if difficulty in the Left Turn condition might relate to the bats' handedness (Zucca et al., 2010).

Beam aim anticipates the turn

A previous experiment quantifying beam aim required big brown bats to fly through an open room or through openings in mist nets to catch a tethered insect prey (Ghose and Moss, 2003; Surlykke et al., 2009). In the open room, bats focused their beam aim on the prey about 300 ms before reaching it, with a beam aim accuracy of around 3° (Ghose and Moss, 2003). When mist nets were introduced, bats sequentially scanned the edges of the openings, with an accuracy of $\pm 5°$, about 100–300 ms before flying through the opening (Surlykke et al., 2009). Bats flying through the Straight corridor in our experiment aimed their sonar beam straight ahead relative to their heading at a similar accuracy.

We hypothesized that bats flying toward abrupt 90° turns would aim their sonar beam in the direction of these turns before reaching them. Our results support this hypothesis. Bats that were able to navigate in the Turn conditions shifted their beam in the appropriate direction between 30 and 65 cm (224–359 ms) before reaching the turns. These anticipatory times are at the upper edge of the time range quantified by Surlykke et al. (2009). We suggest that these longer anticipatory times reflect the increased difficulty of locating the gap in the dense, intense acoustic clutter surrounding it. Even in these successful flights, bats continued to aim a small number of calls straight ahead or toward the opposite side of the corridor, but there was little sequential side-to-side scanning. This pattern, measured from 32,831 biosonar calls, was remarkably consistent across individual bats and flight days. As we also predicted, shifts in the direction of beam aim were related to behavioral performance. In failed flights, bats largely failed to aim their beam in the direction of the turn; instead, they aimed their beam straight ahead, slightly toward the new turn, or toward the previously encountered opposite turn. The few calls aimed in the correct direction indicates that the bats probed both sides of the corridor even though calls are focused in one particular (in this case, incorrect) direction. These data support the hypothesis that it is the failure to switch beam aim that underlies deficits in behavioral performance.

Consistent with the formation of a spatial map (Barchi et al., 2013), bats adjusted their beam to the direction of the turns as they gained more experience with the spatial layout of the flight corridor. All bats initially

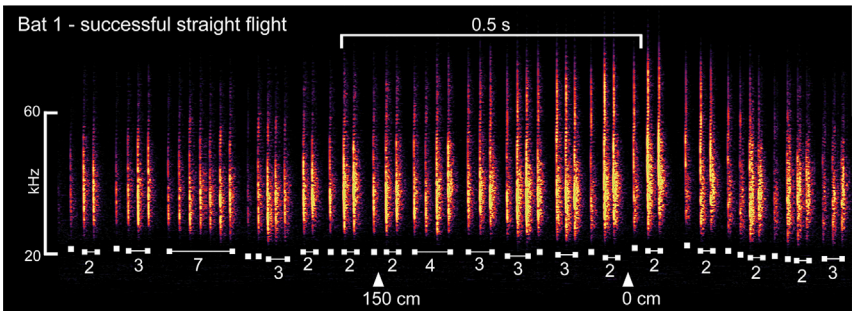

Figure 6. Spectrogram of calls emitted by Bat 1 during a single successful flight through the Straight corridor

SSGs were categorized using the algorithm devised by Kothari et al. (2014) and modified by Warnecke et al. (2016, 2018). White labels and numbers underneath calls identify these SSG categorizations and the number of pulses within each group. White triangles show the bat's position relative to the point at which the position of the turn (at 0 cm) in the Turn conditions (beam 2 in Figure 1). After flying past the 0 cm mark, the bat lowers the frequency of its pulses in preparation for landing on the wall.

failed to switch their beam aim when first introduced to 90° turns, and this was reflected in their poor performance. To increase performance, bats needed to adjust their beam aim to focus on the chains surrounding the turn. For the first day of flights in the new Right Turn condition, two bats continued to aim their beams straight ahead. Two other bats displayed more flexibility, shifting their calls in the direction of the new Right Turn on the first day they were exposed to it. By the end of the Right Turn condition, all bats shifted their beam aim to the correct side and all completed the task successfully. On the first day of Left Turn flights, all bats aimed their beam within $\pm 9°$ of the midline. As the bats gained more experience in this condition, two of them adjusted their beam aim toward the left and successfully completed the task. Two other bats did not adjust their beam aim and failed the task (Figure 4). These data point to considerable individual variability in how flexible bats are when it comes to revising a learned spatial layout.

A strategy of focusing the center of the sonar beam on the nearest obstacle preventing a turn is an adaptive strategy that allows bats to localize and navigate tight spaces, such as gaps in foliage, more accurately. The center of the beam provides the highest signal-to-noise ratio (SNR) for echoes from any potential obstacle compared with the periphery (Ghose and Moss, 2003; Knowles et al., 2015). Focusing its calls on the nearest chain at the "corner" of the turn would allow the bat to perceive the first object to be avoided with a high SNR. However, aiming at the corner chain in the upcoming gap requires perceiving the open gap in the chains before actually reaching the turn, in spite of the intervening chains that prevent flight in the direction of the turn before physically arriving at the turn. For a bat flying at speed, the ability to perceive the two surfaces that define a gap accurately is crucial for localizing and perceiving the spatial properties of that gap, whether the surrounding obstacles are foliage or hanging chains. It is presumably for this reason that in successful turn flights bats focus on the area around the first chain defining the gap. This strategy of focusing the center of their beam on the upcoming obstacle reinforces previous results showing that big brown bats preferentially use the center of their beam to localize and track goal-related objects (Ghose and Moss, 2003; Surlykke et al., 2009), in contrast to other echolocating bats that employ an alternative spatial-sampling strategy to localize targets (Yovel et al., 2010, 2011). The overall conclusion is that the bats were able to perceive the upcoming open gap in the corridor and anticipate the upcoming turn both by slowing down and by aiming their broadcasts into the gap.

Changing beam aim based on an acquired spatial memory of the flightpath is beneficial to bats that must navigate tight spaces, allowing them to collect as much information as possible about upcoming obstacles in the direction of flight. However, an early proactive movement of the beam may make the bat less able to adapt to abrupt changes in the environment, even after multiple encounters with a new flightpath. Bats may incur a perceptual cost by shifting their acoustic gaze too early; a portion of their approach to the turn is spent echolocating off-axis from the area into which they will fly before entering the turn. Any echoes received from this immediately upcoming area would be perceived as clutter and perceptually blurred (Bates et al., 2011), making it difficult to perceive its distance and structure. The bats' built-up spatial memory of the flightpath allows them to incur this perceptual cost for the benefit of spending more time gathering perceptual information about the upcoming gap.

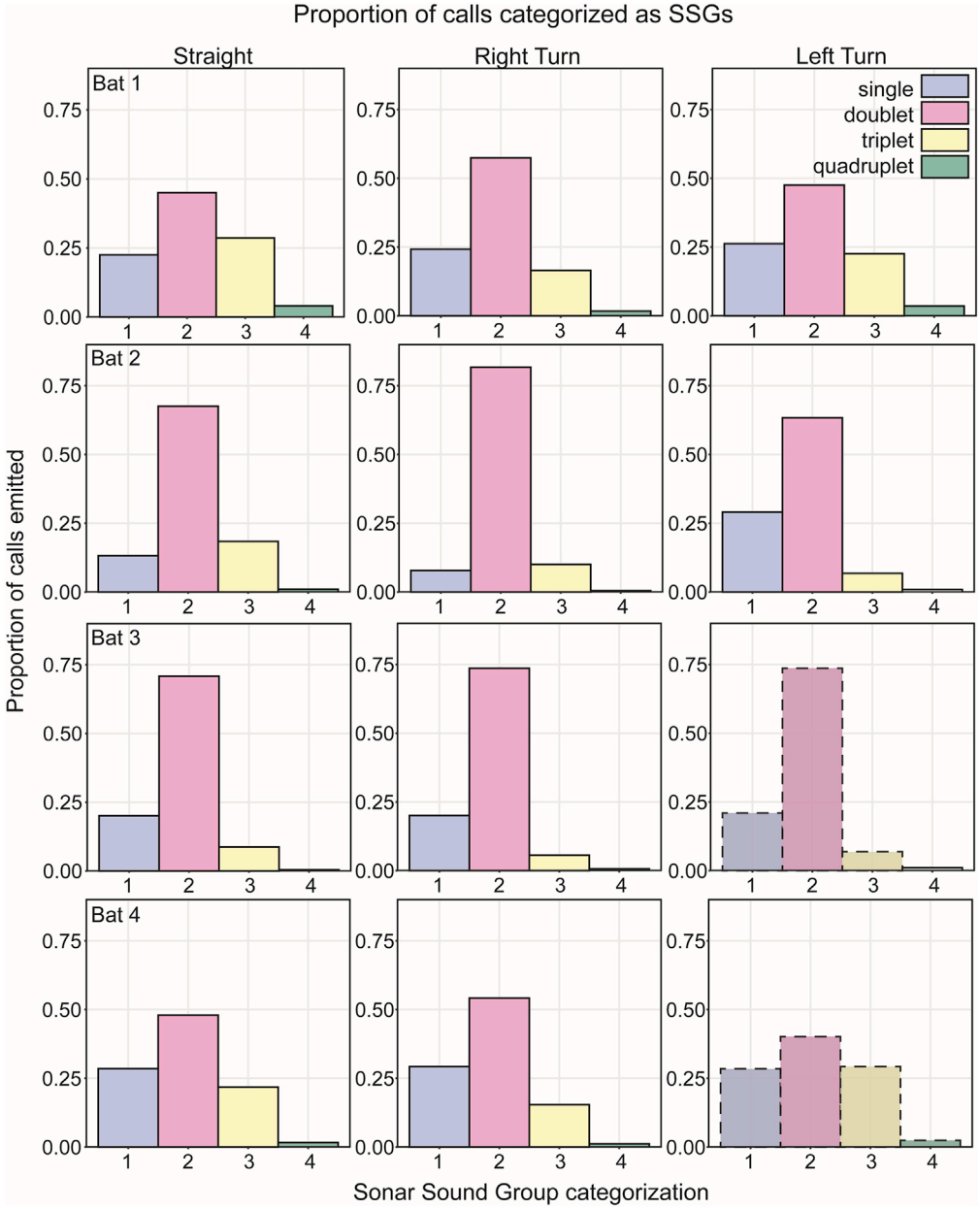

Figure 7. Proportions of calls emitted as Sonar Sound Groups (SSGs)

Bats emitted the majority of their calls in SSGs (as opposed to single calls) in all flight conditions, although the relative proportion varies. SSG of 1 (blue) = single call; 2 (pink) = doublet; 3 (yellow) = triplet; 4 (green) = quadruplet. Solid outlined bars show data from successful flights. The dashed outlined bars (Bat 3 and Bat 4, Left Turn) show failed flights. SSG/single call proportions in Turn flights are significantly different from SSG/single call proportions in Straight flights for all bats (McNemar chi-square tests, $p < 0.001$).

Call timing is related to task difficulty

Insectivorous echolocating bats increase their sensory acquisition rate as background clutter becomes physically closer or denser, and as they approach a landing surface or wall (Falk et al., 2014; Lewanzik and Goerlitz, 2021; Moss et al., 2006; Petrites et al., 2009; Wheeler et al., 2016). The changes in call timing and IPI in our experiment reinforce these earlier findings. Mean IPIs were similar in successful Straight, Right Turn, and Left Turn flights. Bats increased IPIs as they flew down the Straight corridor and as they gained more experience with this flight-path, suggesting that this flight condition was perceptually easier than the Turn conditions. Bats decreased IPIs

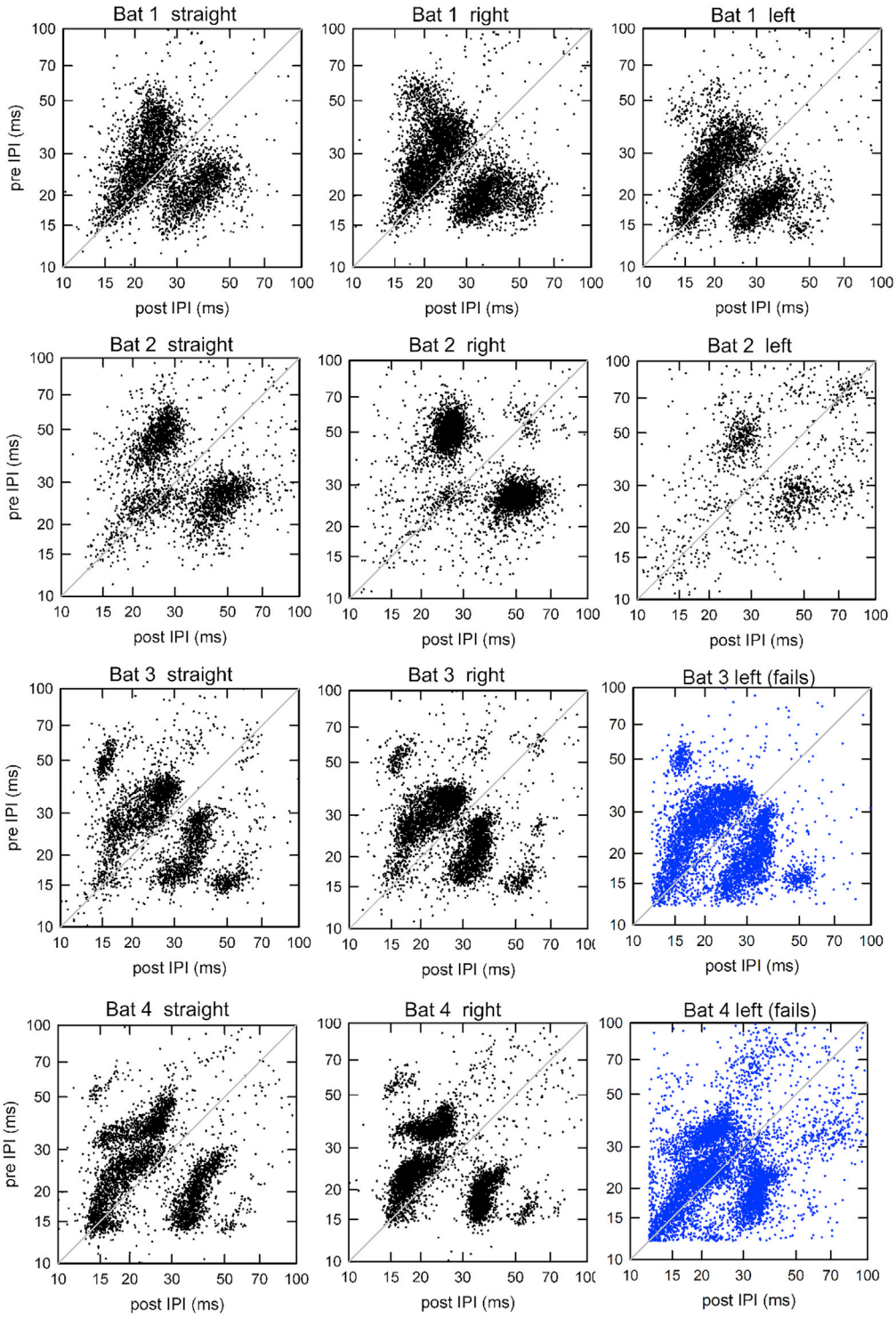

Figure 8. The distribution of pre-IPI and post-IPI of all calls emitted in all flights

Calls along the gray solid diagonal line have equal pre- and post-IPI values. Plots with blue symbols show IPIs in failed Left Turn flights for Bat 3 and Bat 4. Bat 2 in the Left Turn condition emitted fewer calls, so the plot seems less dense. These plots reveal identifiable and consistent qualitative differences in the timing patterns that individual bats employ when navigating through clutter. Note persistence of distinctive plot patterns for each bat across conditions.

as they approached turns in the flightpath, indicating that these flights were more challenging. IPIs decreased more in successful Left Turn than Right Turn flights, highlighting the increased perceptual difficulty of these left turns. Over experimental days, IPIs increased in Straight and Right Turn flights but decreased in Left Turn flights. IPIs also decreased in failed flights. These shorter IPIs again indicate the perceptual difficulty of the Left Turn flights in particular.

We predicted that more calls would be emitted as SSGs in the more difficult Turn conditions, and the data support this prediction. These data are also consistent with previous work showing more call clustering in tasks presumed to be more perceptually difficult (Beetz et al., 2019; Lewanzik and Goerlitz, 2021; Moss et al., 2006; Petrites et al., 2009; Wheeler et al., 2016). SSG production helps the bats alleviate pulse-echo ambiguity created by multiple closely spaced rows of acoustic clutter (Accomando et al., 2018; Knowles et al., 2015; Petrites et al., 2009; Wheeler et al., 2016). In our experiment, the most common SSG was a doublet (mean 61%, range 42%–82% in successful flights in the three conditions). Other experiments in which bats flew down different-sized corridors surrounded by various densities of clutter reported doublets at 62% (Warnecke et al., 2016, 2018) and 37% (Wheeler et al., 2016) of all SSGs. In our experiment, an average of 15% (range 6%–22%) of SSGs were classified as triplets, similar to that found by Wheeler et al. (16%; 2016) but larger than identified in earlier work with FM bats (< 10%; Warnecke et al. [2016];, <5%, Beetz et al. [2019]). Doublets were the most common SSGs emitted in failed Left Turn flights. Two bats that were unable to perform these left turns produced more SSGs than in successful Right Turn flights. We interpret this finding to suggest that bats attempted to update their acoustic scene even under conditions when they did not adjust their beam aim to point toward the correct portion of the corridor.

The visualization of pre/post-IPI distributions for individual bats indicates that individual bats use unique patterns of call timing in order to solve the same perceptual task, and that these unique patterns within individuals are consistent across changes in the surrounding environment. Indeed, the pre-IPI to post-IPI distributions in failed flights were similar to those in successful flights by the same individual. Variability in task performance among bats is not attributable to changes in the temporal patterns of sensory acquisition, but rather due to individual differences in the spatial sampling strategies employed.

General discussion

Together, these findings paint a picture of how bats modify their biosonar behaviors to perceive upcoming obstacles (chains), adjust their calling patterns to avoid these obstacles, and adapt their beam aim to drastic changes in the spatial environment. Bats localizing and navigating a gap within dense acoustic clutter focus their calls on the nearest obstacle defining the edges of the gap in order to best localize the relatively small gap. In effect, they make sonar "looks" into the surrounding clutter to identify upcoming openings amid multiple nearer objects and echoes arriving earlier than the absence of echoes signifying the opening. In this way, they can identify an open flightpath. These proactive beam aim changes are tightly integrated with a spatial memory of the bat's environment, which is built up with experience. This is best exemplified by the persistence of some bats in aiming their calls in the direction required by a previous condition, even after substantial experience in a new spatial layout. This spatial memory, required for successful navigation, may also inhibit the ability of bats to adapt to sudden changes in the environment. Bats that were able to unlearn a pattern of beam aim were more successful in navigating a novel, orthogonal flightpath compared with other bats that became "stuck" in a learned pattern of beam aim. These differences between individual bats could lead to significant differences in their ability to navigate and survive in volatile, physically changing environments. We conclude that failures in navigating complex flightpaths are due to the bat being unable to alter its beam aim, not to an inability to change its sensory acquisition rate. Final success reflects the bat's ability to form a new spatial map of its environment (Barchi et al., 2013).

Limitations of the study

One issue raised by this experiment concerns the poor performance of two of the four bats in the Left Turn condition. It is possible that the Left Turn was more challenging because it was closer to the flight room wall. The simultaneous use of the flight room for other experiments prevented locating the experimental corridor in a more symmetrical manner. The better performance of these two bats in a Reversed Right Turn condition suggests that proximity to the wall did not affect their performance; rather, they did poorly in the Left Turn because they became "stuck" in aiming their beam toward the right. However, this new condition could only be run for one day, because of the bats' refusal to continue flying. These two bats were in good health during the experiment, and remained so for one year after its end. Finally, although the LMM

model controlled statistically for the fixed order of conditions, future experiments should randomize conditions. It is also more difficult to quantify changes in temporal patterning that may have occurred in response to spatial changes, as time spent in the experiment is a confounding factor for all bats.

Resource availability

Lead contact

Further information and requests should be directed to and will be fulfilled by the corresponding author, Andrea Simmons (Andrea_Simmons@brown.edu).

Materials availability

Please contact the corresponding author.

Data and code availability

Original data have been deposited in the Brown Digital Repository: https://doi.org/10.26300/0mpw-9f40.

METHODS

All methods can be found in the accompanying Transparent Methods supplemental file.

SUPPLEMENTAL INFORMATION

Supplemental information can be found online at https://doi.org/10.1016/j.isci.2021.102353.

ACKNOWLEDGMENTS

This research was supported by grants from the Office of Naval Research (N00014-14-1-05880 to J.A.S., N00014-17-1-2736 to J.A.S. and A.M.S). A.T. is supported by a National Science Foundation Graduate Research Fellowship. Meike Linnenschmidt assisted with data collection; Alexandra Ertman, Abigail Kohler, and McKenna Schimmel assisted with data processing.

AUTHOR CONTRIBUTIONS

Conceptualization: K.N.H. and A.M.S.; methodology: K.N.H., A.M.S., and J.A.S.; software: C.M.; formal analysis: A.T. and C.M.; investigation: K.N.H., A.M.S., and J.A.S.; writing – original draft: A.T. and A.M.S.; writing – review & editing: K.N.H., C.M., and J.A.S.; visualization: A.T., C.M., and J.A.S.; supervision: A.M.S. and J.A.S.; project administration: A.M.S. and J.A.S.; funding acquisition: A.M.S. and J.A.S.

DECLARATION OF INTERESTS

The authors declare no competing interests.

INCLUSION AND DIVERSITY

One or more of the authors of this paper self-identifies as an underrepresented ethnic minority in science. While citing references scientifically relevant for this work, we also actively worked to promote gender balance in our reference list.

Received: January 24, 2021
Revised: March 7, 2021
Accepted: March 19, 2021
Published: April 23, 2021

REFERENCES

Accomando, A.W., Vargas-Irwin, C.E., and Simmons, J.A. (2018). Spike Train Similarity Space (SSIMS) method detects effects of obstacle proximity and experience on temporal patterning of bat biosonar. Front. Behav. Neurosci. *12*, 1–14.

Amichai, E., and Yovel, Y. (2017). Bats pre-adapt sensory acquisition according to target distance prior to takeoff even in the presence of closer background objects. Sci. Rep. *7*, 467.

Barchi, J.R., Knowles, J.M., and Simmons, J.A. (2013). Spatial memory and stereotypy of flight paths by big brown bats in cluttered surroundings. J. Exp. Biol. *216*, 1053–1063.

Bates, M.E., Simmons, J.A., and Zorikov, T.V. (2011). Bats use echo harmonic structure to distinguish their targets from background clutter. Science *333*, 627–630.

Beetz, M.J., Kössl, M., and Hechaverría, J.C. (2019). Adaptations in the call emission pattern of frugivorous bats when orienting under

challenging conditions. J. Comp. Physiol. A. *205*, 457–467.

Denny, M. (2007). Blip, Ping & Buzz: Making Sense of Radar and Sonar (Johns Hopkins University Press).

Falk, B., Jakobsen, L., Surlykke, A., and Moss, C.F. (2014). Bats coordinate sonar and flight behavior as they forage in open and cluttered environments. J. Exp. Biol. *217*, 4356–4364.

Fujioka, E., Aihara, I., Watanabe, S., Sumiya, M., Hiryu, S., Simmons, J.A., Riquimaroux, H., and Watanabe, Y. (2014). Rapid shifts of sonar attention by *Pipistrellus abramus* during natural hunting for multiple prey. J. Acoust. Soc. Am. *136*, 3389–3400.

Ghose, K., and Moss, C.F. (2003). The sonar beam pattern of a flying bat as it tracks tethered insects. J. Acoust. Soc. Am. *114*, 1120–1131.

Grief, S., Zsebők, S., Schmieder, D., and Siemers, B.M. (2017). Acoustic mirrors as sensory traps for bats. Science *357*, 1045–1047.

Griffin, D.R. (1958). Listening in the Dark (Yale University Press), reprinted by Cornell University Press, Ithaca, NY, 1986.

Hartley, D., and Suthers, R. (1989). The sound emission pattern of the echolocating bat, *Eptesicus fuscus*. J. Acoust. Soc. Am. *85*, 1348–1351.

Hiryu, S., Bates, M.E., Simmons, J.A., and Riquimaroux, H. (2010). FM echolocating bats shift frequencies to avoid broadcast-echo ambiguity in clutter. Proc. Nat. Acad. Sci. USA *107*, 7048–7053.

Hom, K.N., Linnenschmidt, M., Simmons, J.A., and Simmons, A.M. (2016). Echolocation behavior in big brown bats is not impaired after intense broadband noise exposures. J. Exp. Biol. *219*, 3253–3260.

Knowles, J.M., Barchi, J.R., Gaudette, J.E., and Simmons, J.A. (2015). Effective biosonar echo-to-clutter rejection ratio in a complex dynamic scene. J. Acoust. Soc. Am. *138*, 1090–1101.

Kothari, N.B., Wohlgemuth, M.J., Hulgard, K., Surlykke, A., and Moss, C.F. (2014). Timing matters: sonar call groups facilitate target localization in bats. Front. Physiol. *5*, 1–13.

Kounitsky, P., Rydell, J., Amichai, E., Boonman, A., Eitan, O., Weiss, A.J., and Yovel, Y. (2015). Bats adjust their mouth gape to zoom their biosonar field of view. Proc. Natl. Acad. Sci. USA *112*, 6724–6729.

Lewanzik, D., and Goerlitz, H.R. (2021). Task-dependent vocal adjustments to optimize biosonar-based information acquisition. J. Exp. Biol. *224*, jeb234815.

Melcón, M.L., Yovel, Y., Denzinger, A., and Schnitzler, H.-U. (2011). How greater mouse-eared bats deal with ambiguous echoic scenes. J. Comp. Physiol. A. *197*, 505–514.

Moss, C.F., Bohn, K., Gilkenson, H., and Surlykke, A. (2006). Active listening for spatial orientation in a complex auditory scene. Plos Biol. *4*, 615–626.

Moss, C.F., and Surlykke, A. (2001). Auditory scene analysis by echolocation in bats. J. Acoust. Soc. Am. *110*, 2207–2226.

Petrites, A.E., Eng, O.S., Mowlds, D.S., Simmons, J.A., and Delong, C.M. (2009). Interpulse interval modulation by echolocating big brown bats (*Eptesicus fuscus*) in different densities of obstacle clutter. J. Comp. Physiol. A. *195*, 603–617.

Sändig, S., Schnitzler, H.-U., and Denzinger, A. (2014). Echolocation behaviour of the big brown bat (*Eptesicus fuscus*) in an obstacle avoidance task of increasing difficulty. J. Exp. Biol. *217*, 2876–2884.

Schnitzler, H.-U., and Kalko, E.K.V. (2001). Echolocation by insect-eating bats. Bioscience *51*, 557–569.

Simmons, A.M., Ertman, A., Hom, K.N., and Simmons, J.A. (2018). Big brown bats (*Eptesicus fuscus*) successfully navigate through clutter after exposure to intense band-limited sound. Sci. Rep. *8*, 13555.

Simmons, J.A. (2005). Big brown bats and June beetles: multiple pursuit strategies in a seasonal acoustic predator-prey system. Acoust. Res. Lett. Online *6*, 238–242.

Simmons, J.A., Brown, P.E., Vargas-Irwin, C.E., and Simmons, A.M. (2020). Big brown bats are challenged by acoustically-guided flights through a circular tunnel of hoops. Sci. Rep. *10*, 832.

Simmons, J.A., Eastman, K.M., Horowitz, S.S., O'Farrell, M.J., and Lee, D.N. (2001). Versatility of biosonar in the big brown bat, *Eptesicus fuscus*. Acoust. Res. Lett. Online *2*, 43.

Surlykke, A., and Moss, C.F. (2000). Echolocation behavior of big brown bats, *Eptesicus fuscus*, in the field and the laboratory. J. Acoust. Soc. Am. *108*, 2419–2429.

Surlykke, A., Ghose, K., and Moss, C.F. (2009). Acoustic scanning of natural scenes by echolocation in the big brown bat, *Eptesicus fuscus*. J. Exp. Biol. *212*, 1011–1020.

Warnecke, M., Lee, W.-J., Krishnan, A., and Moss, C.F. (2016). Dynamic echo information guides flight in the big brown bat. Front. Behav. Neurosci. *10*, 81.

Warnecke, M., Macías, S., Falk, B., and Moss, C.F. (2018). Echo interval and not echo intensity drives bat flight behavior in structured corridors. J. Exp. Biol. *221*, jeb191155.

Wheeler, A.R., Fulton, K.A., Gaudette, J.E., Simmons, R.A., Matsuo, I., and Simmons, J.A. (2016). Echolocating big brown bats, *Eptesicus fuscus*, modulate pulse intervals to overcome range ambiguity in cluttered surroundings. Front. Behav. Neurosci. *10*, 1–13.

Yovel, Y., Falk, B., Moss, C.F., and Ulanovsky, N. (2010). Optimal localization by pointing off axis. Science *327*, 701–704.

Yovel, Y., Geva-Sagiv, M., and Ulanovsky, N. (2011). Click-based echolocation in bats: not so primitive after all. J. Comp. Physiol. A. *197*, 515–530.

Zucca, P., Palladini, A., Baciadonna, L., and Scaravelli, D. (2010). Handedness in the echolocating Schreiber's long-Fingered bat (*Miniopterus schreibersii*). Behav. Proc. *84*, 693–695.

iScience, Volume *24*

Supplemental information

Spatiotemporal patterning of acoustic gaze in echolocating bats navigating gaps in clutter

Amaro Tuninetti, Chen Ming, Kelsey N. Hom, James A. Simmons, and Andrea Megela Simmons

Key Resources Table

REAGENT or RESOURCE	SOURCE	IDENTIFIER
Deposited data		
Raw and analyzed data	This paper	https://doi.org/10.26300/0mpw-9f40
Experimental models: organisms/strains		
Big brown bats, *Eptesicus fuscus*	Wild-caught	NA
Software and algorithms		
MATLAB	MathWorks, Natick MA	Version 2018a
SPSS	IBM Corp, Armonk NY	Version 25
R Studio	Rstudio.com	2020, Version 3.6.3
GraphPad	GraphPad Software, San Diego CA	Version 9.0.0
Other		
Electret microphones	Knowles Electronics, Itasca IL	SMG-0291
Data acquisition system	Astro-Med, West Warwick RI	DMX-8000

Transparent Methods

Animals

Animal care and experimental procedures were approved by the Brown University Institutional Animal Care and Use Committee and adhere to federal guidelines. Four adult big brown bats (three males, one female) were captured from barns in Rhode Island USA, authorized by a scientific collecting permit from the state of Rhode Island. Because these bats were wild-caught, their ages are not known. All bats flew and echolocated normally, as recorded in exercise flights conducted in an empty flight room. Animals were group-housed in a temperature- and humidity-controlled colony room (22-24° C, and 40-60% relative humidity) on a reverse 12:12 dark/light cycle. Individuals were identified by unique haircuts on their back fur. Bats had unlimited access to vitamin-enriched water in their home enclosures and received their daily food allotment (live mealworms, *Tenebrio* larvae) during experiments as rewards for successful performance. If they did not obtain the total food allotment during experiments because of poor performance, they were fed subsequently in their home enclosures. Two animals (Bat 1 and Bat 4) participated in previous experiments that involved flying through chain arrays of varying densities and configurations but lacking abrupt spatial changes (Hom et al., 2016; Simmons et al., 2018; Wheeler et al., 2016); two other animals (Bat 2 and Bat 3) were naïve to flight experiments.

Flight Room

Flights took place in a custom-built flight room (8.3 m × 4.3 m × 2.7 m; Figure 1) lined with acoustically and electrically insulated sound-absorbent foam (SONEX "One" acoustic panels; Pinta Acoustics, Minneapolis, MN USA) on the ceiling and walls. The floor was lined with carpet to help attenuate echoes. Black plastic chains (217 total; link size 4.0 cm wide, 7.5 cm long, 1.0 cm thick) were suspended from cross bars in the ceiling and extended to the floor to create a straight, 5 m long, 40 cm wide corridor. These chains reflect intense echoes (87-97 dB SPL re 20 μPa as measured by Petrites et al., 2009) that are extended in time, and are analogous to echoes reflected by dense vegetation. Chains were arranged in rows and columns 20 cm apart and were weighted on the floor end to keep them from swaying. This is a denser arrangement than in earlier experiments (Hom et al., 2016; Petrites et al., 2009; Wheeler et al., 2016) and was chosen in order to prevent bats from easily flying out of the experimental flightpath when it was abruptly changed. In the plan diagram of the flight room (Figure 1), filled circles show the positions of hanging chains and open circles show the position of chains removed to construct different corridor configurations (Straight, 90° Left Turn, 90° Right Turn, Reversed Right Turn). The chain array is not located symmetrically in the flight room because it was constrained by equipment needed for unrelated experiments. When the bat turned to the right, it had a farther distance to fly to Wall C then when it turned left towards Wall A. This lack of symmetry led to the inclusion of a Reversed Right Turn condition.

Two thermal video cameras (v1 and v2) and 16 ultrasonic microphones (numbered boxes, Figure 1) were used to monitor the bat during the experiment. The thermal infrared cameras (Merlin mid-range Photon 320, FLIR Systems, Boston, MA USA) were placed at the beginning of the flight corridor aiming down its length, and in the middle of the corridor facing the floor. Thermal video feeds were used for live monitoring of the bat's flight. Fifteen ultrasonic microphones (SMG-0291 electret microphones, Knowles Electronics, Itasca, IL USA) were placed on Walls A, B, and C, and one (#16) on the ceiling above the turning point (or the corresponding point in Straight flights), to create a microphone array capturing the bat's echolocation calls as it flew. The wall microphones were mounted 0.5, 1.2, 1.6, or 2.1 m above the ground, in an alternating high-low order. This array was used to calculate the bat's position within the corridor at the time of emission of each individual call as well as the direction in which the call was emitted.

To ensure that the bats were not relying on any visual cues to navigate the corridor, flights took place in full darkness, though the room was illuminated by infrared LEDs mounted on the walls for video recording and monitoring purposes.

Supplemental Experimental Procedure

Flights were conducted by three experimenters. Experimenter 1 was responsible for releasing the bats at the start of the corridor, retrieving them when they landed on the wall, and then rewarding them for successful flights. Experimenter 2 turned on the acoustic recording equipment prior to the bat's release

and stopped the equipment when the bat landed on the back wall, while Experimenter 3 took notes on each flight.

Bats were exposed to different corridor configurations (flight conditions) in a fixed order. The experiment began with 7 days of flights through the Straight corridor. All bats then completed 9 days of flights in the Right Turn condition (towards Wall C) and finally 6-7 days of flights in the Left Turn condition (towards Wall B). Two bats were tested for one day in a Reversed Right Turn condition, being released from Wall B to find the gap leading towards Wall A. Each bat completed 15-18 flights per day, with the goal of 15 successful flights.

Data analysis

Performance

The data collected from each flight consisted of ultrasonic recordings of the bat's echolocation calls and its performance (success or failure). Any flight in which the bat successfully flew from the beginning of the corridor to the appropriate wall without looping back to the release point, landing on a chain, exiting the corridor through the chains, or falling to the floor was labeled a success and rewarded with a mealworm. Any flight where the bat landed on the floor or on a chain, looped back to the release point without completing the flightpath, flew through the chains, or refused to fly was labelled a failure. Bats were not rewarded for failed flights.

Calculation of flightpath, beam aim, and flight speed

Recordings from all 16 microphones were digitized in real time at a 192 kHz sampling rate using a commercial multichannel data-acquisition system (DMX-8000, Astro-Med Inc., West Warwick, RI USA) and archived in the recording system's dedicated computer. For off-line analysis, they were recovered from the archived format, converted to mono .wav files, and bandpass filtered from 15-75 kHz to remove background noise unrelated to the bat's calls and exploit the strongest part of the signals relative to background noise in the room. This frequency band was used to estimate arrival-time differences at the microphones. Calls recorded from multiple microphones started on the same clock at known positions were cross-correlated to determine the time-difference-of-arrival between channels and the locus of the source for each individual call (Barchi et al., 2013; Gillette and Silverman, 2008; Wei and Ye, 2008). For an individual call to be analyzed, we required that the call be successfully identified on the recordings of seven wall microphones. This threshold was chosen to provide an accurate reconstruction of the location and beam aim of each call while also maximizing the number of calls emitted that could be used for beam aim analysis. The number of channels used to localize a call ranged from 7 to 16, depending on the emitted strength and recording quality of each call.

Beam aim and flightpaths were calculated using custom MATLAB scripts (R2018a, MathWorks, Cambridge, MA USA). For cross-correlation, a single call from each flight was chosen as a reference call. Selecting an intact and strong representation of a bat's call as reference is critical to the accuracy of tracking. Most of the calls emitted within a flight encountered several rows of chains before being recorded by a wall microphone, which results in recordings that can be degraded and contain many spectral notches. However, the directly received call was stronger than the scattered sound, which, being weaker, did not affect the principal peak of the cross-correlation. The microphones nearest the entrance of the corridor (#14 and #15) were able to record initial calls at relatively high amplitudes that were not highly scattered. In some flights, calls reaching these microphones were overly scattered or captured off-axis from the bat, resulting in recordings of calls missing the second harmonic. In these cases, a recorded call from the ceiling microphone (#16) was used as the reference call for that flight, as calls reaching that microphone were not highly scattered by chains.

Once individual calls were localized within the flightpath, the horizontal direction (azimuth) of each call's broadcast beam was calculated. While localization was performed by time-of-arrival measurements using the full band of the FM calls (15-75 kHz), with no role for amplitude or intensity estimates affecting the time values, determining beam aim depends on locating the direction of maximum amplitude using signals recorded by multiple microphones. To mitigate the potential for distortion of beam aim estimates caused by the scattering effect of the chains on any particular microphone's estimate of call amplitude, we bandpass filtered (equiripple FIR filter) the calls to 30-32 kHz. This frequency band is strongly

represented in big brown bat echolocation calls, and these lower frequencies travel more effectively than the higher frequencies in the full call bandwidth without being scattered by the 1.0 cm thick loops on the chains. The intensity of a call at each microphone was obtained by squaring the bandpass filtered signal to obtain its envelope and then integrating this squared envelope to arrive at a single intensity value for that call. After correcting the signal intensity at each microphone for spherical loss and atmospheric attenuation incurred over the path length from the location of the call, the beam axis of each call was calculated by summing all direction vectors whose lengths are proportional to the corrected intensity to find the central axis of the beam (Ghose and Moss, 2003). A total of 14 microphones was used in the beam aim calculation. Microphone #10 was excluded because in a large number of flights the recording from this microphone appeared abnormal, likely due to a bad connection at the time of experiments; microphone #16 was placed centrally on the ceiling and thus did not provide azimuthal information.

To quantify trends in beam aim during each flight, we averaged beam angle across overlapping windows of the flight corridor. The section of corridor preceding the 90˚ turn was divided into 10 cm windows. The mean and SD of beam aim angle was calculated for all pulses emitted within that window. Mean beam aim was determined to deviate from the midline in turn conditions when the SD of beam aim angles across all emitted calls no longer overlapped the 0˚ line (facing straight ahead in the chain array).

Flight speeds on successful flights were calculated from the pulse timing and localization data using custom MATLAB scripts. Speed in each of two segments of the corridor, as referred to the position of the turn at 0 cm (speed 1, 250 – 100 cm; speed 2, 100 – 0 cm; orange and purples lines, respectively, in Figure 1), was computed by selecting the calls that most closely corresponded to the Y-positions of the selected ranges, and calculating the corresponding time-lapse between selected calls. The nearer segment (100 – 0 cm before the turn) was chosen because individual bats diverted their beam angle away from the midline at various points between 100 – 0 cm from the turn (see Figure 4), meaning the bats began physically preparing for the turn within 100 cm from the turn. The farther segment (250 – 100 cm) was chosen as the comparison range because this segment was most representative of the bat's stable flight speed in the straight section of the turn conditions. Distances farther than 250 cm from the turn were excluded to avoid variable flight speeds due to the bat's initial release. Failed flights were excluded. Speeds greater than 5 m/s most likely are errors caused by reflections from the chains and were also excluded. No videos showed bats flying the array length in under 1 s, which would happen at such high speeds. We compared speed distributions in the two corridor segments for each individual bat using two-tailed Kolmogorov-Smirnov tests.

Temporal pattern of call emissions

We calculated numbers of calls and time intervals between individual calls (interpulse intervals, IPI) from the time the bat entered the corridor to the time it reached the turn or equivalent point in Straight flights. An amplitude threshold was set in MATLAB to isolate individual pulses from background noise and to calculate the time-of-occurrence of each pulse. Because different bats emitted calls at different energy levels, the amplitude threshold differed between bats but was kept the same to analyze individual flights from the same bat. To avoid including echoes rather than emitted pulses in the analysis, a minimum time of 10 ms between individual pulses was set. In addition, IPIs > 100 ms were excluded, as these indicate that the bat is not in the corridor. The time between amplitude maxima of pulses was calculated to determine IPI. Sonar sound groups (SSGs) were classified as singles, doublets, triplets, quadruplets, and more based on differences in IPI within groups and between groups of pulses. Classification was done by analyzing IPI values with the algorithm presented in Kothari et al. (2014), with modified criteria (stability criterion = 8%, island criterion = 1.1; Warnecke et al., 2016, 2018) developed to account for greater densities of acoustic scenes. The algorithm was run without a maximum SSG size, so as to let the algorithm classify SSGs of any size based on algorithm criteria. SSG classifications were visually confirmed to ensure algorithm criteria did not produce false positives. The temporal patterning of calls was visualized by plotting the distribution of calls that were classified as SSGs, plotting the results of linear mixed effects models showing how IPI changed over flight time, and plotting pre-IPI against post-IPI for calls emitted in flight (Wheeler et al., 2016).

Statistical analyses

Performance data were analyzed by repeated measures analysis of variance (ANOVA; SPSS v. 25), with bat as the random factor and condition (Straight, Right Turn, Left Turn) as the fixed factor. The distance at which beam aims shifted in the direction of a turn was determined by when the SD of beam aims in a window no longer overlapped the flight path's midline (0˚). Beam shift linear regressions from the first and last day of flights were compared with ANCOVA pairwise comparisons (Bonferroni-corrected α = 0.004; GraphPad Software v9.0.0).

We analyzed IPIs using linear mixed effects models (LMM) using the *lmer4* package in RStudio (2020, R version 3.6.3). Mixed effects models account for the hierarchical repeated-measures structure of the data (each individual bat emits *n* calls, resulting in *n*-1 IPIs, on flight *x*, on day *y*, of condition *z*) as well as datasets of unequal *n* without discarding data. The variables Bat, Flight Number, Day Number, and Condition were included as nested random effects. The hierarchical random effects structure of the first LMM helps account for the fact that all bats completed the different flight conditions in the same, as opposed to randomized, order (Straight, Right Turn, Left Turn) and for several consecutive days each. In this LMM, three fixed effects were included: Condition, the Number of Calls remaining before reaching the turn, and the interaction between those two effects. The number of calls remaining before the bat reached the turn was used to estimate how close the bat was to entering the turn (or the equivalent point in Straight flights). Precise physical distance from the turn is not known for every single call, as precise localization of the bat required a call to be picked up by seven microphones. Thus, we identified the final call that was successfully localized as being emitted before the entrance to the turn, and indexed the number of calls remaining (before reaching the turn) backwards from the final call. To test whether changes in IPI while approaching the turn were different across the three conditions, pairwise comparisons of the condition*calls-to-turn interaction were performed by contrast coding in order to compare IPI slopes in the Right and Left Turn flights to the slope in Straight flights (Wendorf, 2004). Significance of effects and pairwise comparisons was determined using the *lmerTest* package in RStudio, which performs F tests using Satterthwaite's degrees of freedom method (Brown, 2020).

We fit IPI data to a second LMM quantifying how IPI changed over the course of 7-9 days of flying in the same configuration of chains, as each bat flew within a single configuration for 7-9 continuous days before switching to another chain configuration. This LMM differs in two ways from the previous IPI model. First, it replaces the fixed effect of Number of Calls to turn with a fixed effect of Number of Days, which quantifies how many consecutive days the bat has been flying in a condition. Second, the fixed effect interaction is now between Condition and Number of Days (rather than Number of Calls).

To test for changes in SSGs, we used McNemar repeated-measures chi-squared tests (SPSS, v. 25) to determine if, when introduced to a new task condition, bats significantly changed the proportion of calls they emitted as single calls and the proportion of calls they emitted as parts of an SSG.

Supplemental References

Barchi, J. R., Knowles, J. M., and Simmons, J. A. (2013). Spatial memory and stereotypy of flight paths by big brown bats in cluttered surroundings. J. Exp. Biol. *216*(6), 1053–1063. https://doi.org/10.1242/jeb.073197

Brown, V. A. (2020, April 11). An introduction to linear mixed effects modeling in R. https://doi.org/10.31234/osf.io/9vghm

Ghose, K. and Moss, C. F. (2003). The sonar beam pattern of a flying bat as it tracks tethered insects. J. Acoust. Soc. Am. *114*(2), 1120–1131. https://doi.org/10.1121/1.1589754

Gillette, M. D. and Silverman, H. F. (2008). A linear closed-form algorithm for source localization from time-differences of arrival. IEEE Signal Process. Lett. *15*, 1–4. https://doi.org/10.1109/LSP.2007.910324

Hom, K. N., Linnenschmidt, M., Simmons, J. A., and Simmons, A. M. (2016). Echolocation behavior in big brown bats is not impaired after intense broadband noise exposures. J. Exp. Biol. *219*, 3253-3260.

https://doi.org/10.1242/jeb.143578

Kothari, N. B., Wohlgemuth, M. J., Hulgard, K., Surlykke, A., and Moss, C. F. (2014). Timing matters: Sonar call groups facilitate target localization in bats. Front. Physiol. *5*, 1–13. https://doi.org/10.3389/fphys.2014.00168

Petrites, A. E., Eng, O. S., Mowlds, D. S., Simmons, J. A., and Delong, C. M. (2009). Interpulse interval modulation by echolocating big brown bats (*Eptesicus fuscus*) in different densities of obstacle clutter. J. Comp. Physiol. A *195*(6), 603–617. https://doi.org/10.1007/s00359-009-0435-6

Simmons, A. M., Ertman, A., Hom, K. N., and Simmons, J. A. (2018). Big brown bats (*Eptesicus fuscus*) successfully navigate through clutter after exposure to intense band-limited sound. Sci. Rep. *8*, 13555. DOI:10.1038/s41598-018-31872-x

Warnecke, M., Lee, W-J., Krishnan, A., and Moss, C. F. (2016). Dynamic echo information guides flight in the big brown bat. Front. Behav. Neurosci. *10*, 81. doi: 10.3389/fnbeh.2016.00081

Warnecke, M., Macías, S., Falk, B., and Moss, C. F. (2018). Echo interval and not echo intensity drives bat flight behavior in structured corridors. J. Exp. Biol. *221*, jeb191155, 2018. doi:10.1242/jeb.191155

Wei, H.-W., and Ye, S.-F. (2008). Comments on 'A linear closed-form algorithm for source localization from time-differences of arrival'. IEEE Signal Processing Letters *15*, 895–895. https://doi.org/10.1109/LSP.2008.2001113

Wendorf, C. A. W. (2004). Primer on multiple regression coding: Common forms and the additional case of repeated contrasts. Understanding Statistics, *3*(1), 47-57.

Wheeler, A. R., Fulton, K. A., Gaudette, J. E., Simmons, R. A., Matsuo, I., and Simmons, J. A. (2016). Echolocating big brown bats, *Eptesicus fuscus*, modulate pulse intervals to overcome range ambiguity in cluttered surroundings. Front. Behav. Neurosci. *10***,** 1–13. https://doi.org/10.3389/fnbeh.2016.00125

Figure S1. **Beam angles in failed flights.** Related to Figure 4.
Beam aim is calculated in the segment of the flight path from 150 cm – 0 cm to the turn (or equivalent point in Straight flights; beam 2 in Figure 1). Empty cells indicate no data for that condition. In failed Left Turn flights, Bat 3 and Bat 4 continued to (mistakenly) aim their beams towards the right as they approached the turn.

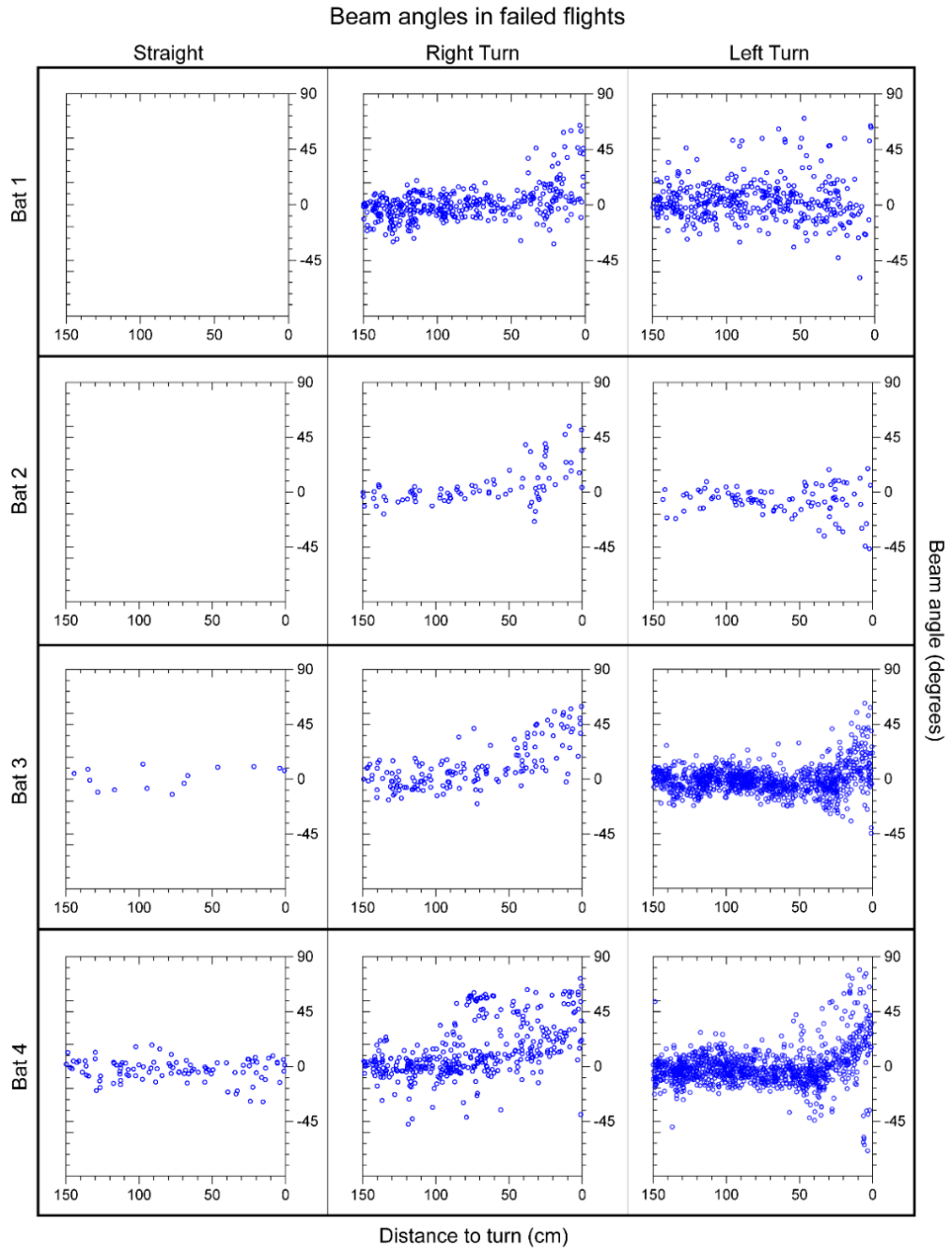

Figure S2. Flight speeds in successful flights. Related to Figure 1 and Figure 4.
Speeds were calculated separately in two segments of the corridor (Figure 1): 250 – 100 cm prior to the turn (speed 1, orange bars), and 100 – 0 cm prior to the turn or equivalent point in straight flights (speed 2, purple bars). Columns (left to right) show data for Straight, Right Turn, and Left Turn flights. Flight speeds in failed flights were not calculated.

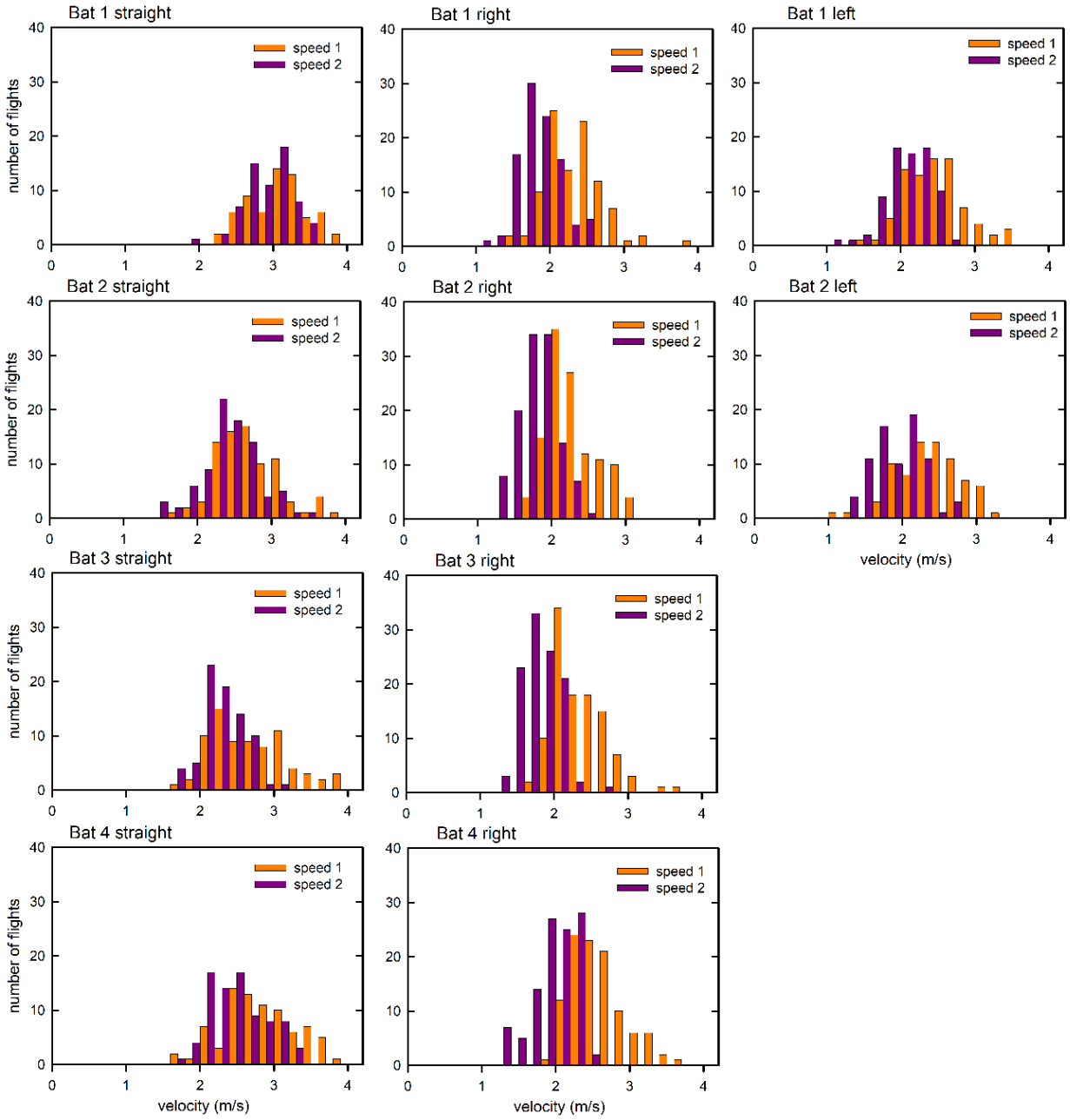

Figure S3. **Spectrograms of calls during a successful (top panel) and a failed (bottom panel) flight through the Right Turn corridor.** Related to Figure 6.
Data are from Bat 1. White labels and numbers identify SSG categorizations and the number of pulses within each group. White triangles with distance measurements indicate the bat's position relative to the upcoming turn (beam 2 segment in Figure 1). In the failed Right Turn flight, the bat failed by colliding with the chains blocking the entrance to the turn (note the buzz-like call structure leading up to the turn).

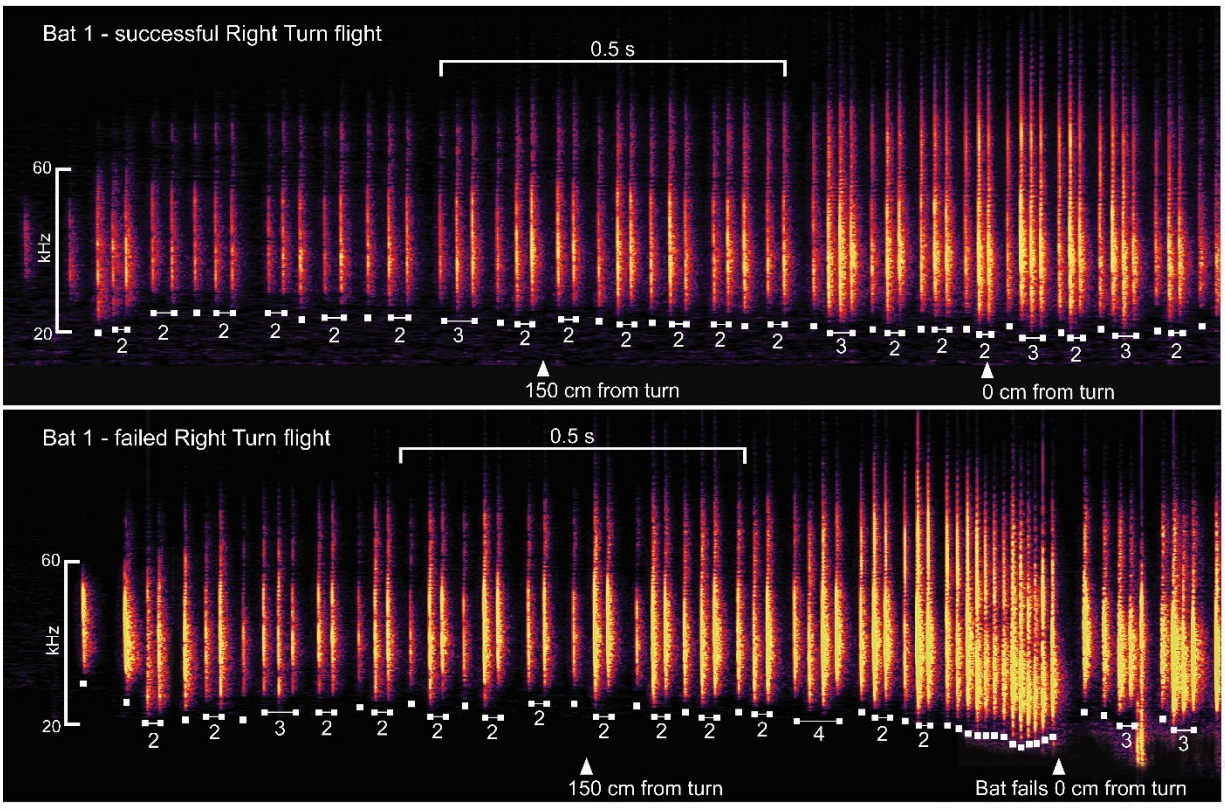

Table S1. **Mean beam angles of calls on failed flights**. Related to Table 1.
Beam angles are calculated for two segments of the corridor (beam 1, 300 – 150 cm; beam 2, 150 – 0 cm; see Figure 1), referenced to distance to the turn. N = number of angles (followed by the number of flights in parentheses), M = mean, SD = standard deviation. Empty cells indicate no data from failed flights for that combination of bat and condition. Italicized values highlight those from the two bats that were experienced in flight tasks.

Condition	**Distance to turn**		***Bat 1***	**Bat 2**	**Bat 3**	***Bat 4***
Straight	300 – 150 cm	**N [calls (flights)]**		11 (2)	14 (4)	*150 (8)*
		M		4.69°	8.91°	*2.27°*
		SD		12.75°	19.83°	*10.95°*
	150 – 0 cm	**N [calls (flights)]**			14 (2)	*47 (5)*
		M			1.92°	*4.98°*
		SD			8.64°	*4.16°*
Right Turn	300 – 150 cm	**N [calls (flights)]**	*622 (27)*	78 (8)	202 (20)	*487 (22)*
		M	*-0.98°*	-1.16°	3.37°	*3.61°*
		SD	*9.06°*	6.47°	11.22°	*8.57°*
	150 – 0 cm	**N [calls (flights)]**	*220 (27)*	66 (8)	117 (20)	*280 (20)*
		M	*16.39°*	22.22°	25.41°	*23.42°*
		SD	*20.43°*	19.87°	22.26°	*20.87°*
Left Turn	300 – 150 cm	**N [calls (flights)]**	*505 (20)*	46 (8)	1011 (80)	*1351 (72)*
		M	*4.80°*	-2.80°	0.90°	*-0.94°*
		SD	*10.64°*	6.83°	7.89°	*9.57°*
	150 – 0 cm	**N [calls (flights)]**	*238 (20)*	38 (8)	539 (76)	*1221 (67)*
		M	*14.17°*	10.59°	12.71°	*25.02°*
		SD	*14.97°*	12.19°	14.87°	*18.18°*

Table S2. Proportions of all calls categorized as SSGs of varying size. Related to Figure 7. SSG size (left column) varies from 1 (single calls) to 8 (octuplets). SSGs were classified using the algorithm used by Warnecke et al. (2016, 2018). The values from Bat 3 and Bat 4 in the Left Turn condition (italicized columns) are based on failed flights only; all other values are based on successful flights only. Proportions of single calls/SSGs in the Turn conditions are significantly different from proportions in the Straight condition (McNemar repeated-measures chi-square tests, all *P* values < 0.001).

	Bat 1			**Bat 2**			**Bat 3**			**Bat 4**		
SSG size	Straight	Right Turn*	Left Turn*	Straight	Right Turn*	Left Turn*	Straight	Right Turn*	*Left Turn**	Straight	Right Turn*	*Left Turn**
1	0.224	0.242	0.261	0.131	0.078	0.288	0.201	0.200	*0.218*	0.284	0.293	*0.271*
2	0.448	0.573	0.474	0.672	0.817	0.627	0.708	0.735	*0.629*	0.478	0.541	*0.393*
3	0.284	0.165	0.225	0.183	0.100	0.067	0.087	0.056	*0.121*	0.217	0.154	*0.277*
4	0.040	0.017	0.036	0.009	0.005	0.008	0.004	0.007	*0.027*	0.017	0.012	*0.041*
5	0.003	0.003	0.002	0.004	0.000	0.003	0.000	0.001	*0.004*	0.002	0.001	*0.009*
6	0.000	0.000	0.002	0.000	0.000	0.003	0.000	0.000	*0.000*	0.001	0.000	*0.004*
7	0.002	0.000	0.000	0.000	0.000	0.000	0.000	0.000	*0.000*	0.000	0.000	*0.004*
8	0.000	0.000	0.000	0.000	0.000	0.004	0.000	0.000	*0.000*	0.000	0.000	*0.000*